CoA Note No. 118

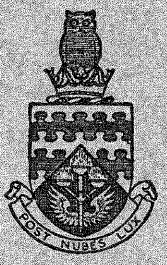

THE COLLEGE OF AERONAUTICS

CRANFIELD

SOME DESIGN PROBLEMS OF THIN SHELL STRUCTURES

- by -

D. J. Johns

NOTE NO. 118

September, 1961.

THE COLLEGE OF AERONAUTICS

CRANFIELD

Some Design Problems of Thin Shell Structures

- by -

D. J. Johns, M.Sc.(Eng.), M.I.Ae.S.

(Paper presented at the 'Seminar on Astronautics'
University of Southampton, 12th-19th July, 1961)

Summary

Simplified analyses are presented which illustrate some of the design problems of typical space vehicle structures, with the emphasis on thin, circular cylindrical shells. Amongst the problems considered are panel flutter, thermal buckling and buckling under axial compression.

CONTENTS

NOTATION

C	r/R
D	Flexural rigidity; diameter
E	Young's modulus
f	Frequency
F	Axial compressive force
ℓ	Head of liquid in vertical shell
L	Length of shell between supports
M	Mach No; Bending moment
m, n	Number of axial half waves and circumferential full waves
N	Longitudinal acceleration
p	Internal gas pressure
r	Minor semi-axis of ellipsoid
R	Major semi-axis of ellipsoid; radius of cylinder
t	Thickness of shell
T	Time; temperature
U	Velocity of airflow
u, v, w	Shell axial, circumferential and radial displacements
W	Weight
x	Axial co-ordinate along shell
Z	Effective lateral pressure on shell
Z_1, Z_2	Time parameters in Section 4
α_c; α	Coefficient of thermal expansion; $^{\omega}/R$ - weight parameter
μ	$\left[Et/4DR^2\right]^{\frac{1}{4}}$
ν	Poisson's ratio
ρ	Density of airflow
ρ_i	Density of liquid in shell

Notation (Continued)

σ_{crit}	Critical axial stress
σ_{max}	Maximum hoop stress
σ_{ϕ}	Thermal hoop stress
ω	Shell mass per unit surface area
Ω	Flutter frequency
λ	$F/\pi R^2$
ϕ	Shell circumferential co-ordinate

Suffices

p	Propellant
o	Initial value
c	Cylinder
s	Sphere
F	Fuel all-burnt

1. Introduction

The purpose of this paper is to make a study of some of the design problems of thin shell structures typical of those employed in space vehicles. Up to the present time all space launching vehicles have consisted of staged chemical rockets in a cylindrical configuration and inspection of some of the more sophisticated design studies for space stations, space probes, etc., has shown that thin cylindrical shells will be prominent as primary structural components. The major emphasis therefore is on the thin circular cylindrical shells typical of current liquid fuelled launching vehicles.

The principal loading actions concerned in the design of space vehicle structures may be separated into the following six phases of interest:

(a) Handling)	
(b) Pre-launch)	Ground loads
(c) Launch)	
(d) In space)	Flight loads
(e) Re-entry)	
(f) Landing)	Impact loads.

Whilst some consideration is given to the 'ground' and 'impact' loading actions the greatest concern is with the flight loads. The main 'in flight' loading cases which are expected to govern the design of the launching vehicle, space vehicle and re-entry vehicle can be conveniently subdivided as follows:-

(a) Pressurisation loads
(b) Axial (e.g. Thrust) loads
(c) Lateral loads
(d) Thermal effects
(e) Dynamic effects
(f) Space environment effects.

Some of these problems will be considered in detail and simplified analyses presented illustrating typical effects and results.

The paper ends with a brief discussion of some specific design studies for space vehicles, and particular emphasis is placed on the prospects for inflatable structures.

2. Pressurisation Loads

Internal pressure loads in space vehicle structures can be expected for the following reasons:-

(1) Hydrostatic pressures in propellant tanks.
(2) Gas pressures for propellant handling purposes.
(3) Structural stabilisation of thin shells.
(4) To provide artificial environment in cabins of manned vehicles or in cargo or instrument compartments.
(5) For compressed gas storage vessels.
(6) In propulsion system components.

It is from considerations such as these that Gerard[1] has suggested that for space craft approximately two thirds of the structure weight could be governed by tension considerations. For ballistic missiles and launching vehicles the proportion may be one half.

Since propellant containers form such a large percentage of the total weight of launching vehicles they have received considerable attention from analysts attempting to achieve structural optimisation. The lightest gas pressure vessel for a given volume is of course the spherical shell and Fig. 1 shows the weight ratio of cylindrical tanks with various fineness ratios as compared to a spherical shell of the same material having the same volume, internal pressure, and maximum stress. The cylinders are assumed to have ellipsoidal ends with the parameter $C = \frac{r}{R}$ defining the ratio of minor to major semi-axes. The lightest cylinder for $C < 1$ has a hemispherical end, $C = 1$.

In deriving Fig. 1 the localised welding stresses caused in manufacture and the discontinuity stresses caused at the cylinder-end junctions have been neglected. Inclusion of these effects would tend to make the cylinders heavier. The equation from which Fig. 1 was obtained is due to Meissner (Ref. 2),

$$\frac{W_c}{W_s} = \frac{4\frac{L}{D} + \frac{1}{C} - C\left\{4 - \frac{1}{2}\left(\frac{1}{1-C^2}\right)^{\frac{1}{2}} L_n \cdot \frac{1+\sqrt{1-C^2}}{1-\sqrt{1-C^2}}\right\}}{3\frac{L}{D} - C} \qquad (2.1)$$

and if $C = 1$, $\frac{W_1}{W_s} = \frac{4\frac{L}{D} - 2}{3\frac{L}{D} - 1}$ (2.2)

Note that if $C = 0.811$, $\frac{W_c}{W_s}$ is independent of $\frac{L}{D}$ and equal to $\frac{4}{3}$. Therefore for $C > 0.811$ greater efficiency is obtained with a lower value of $\frac{L}{D}$.

Although the single sphere may be the lightest pressure vessel, difficulties arise when a series of them are attached together. In order to transmit direct loads through the structure and to provide aerodynamic cleanness, the various pressure vessels will probably be joined by cylindrical connections of the same diameter. Assuming that this connection has the same thickness as the cylindrical portion of the pressure vessels - which are assumed to have hemispherical ends - we find that the higher fineness ratio cylinders have a lighter weight than a system made up of a series of inter-connected spheres. The relevant formula is

$$\frac{W_1}{W_s} = \frac{4}{9}\left[\frac{2\frac{L}{D} + 1}{2\frac{L}{D} - \frac{2}{3}}\right], \qquad (2.3)$$

shown in Fig. 2.

The smallest value of this ratio $\frac{W_1}{W_s} = \frac{4}{9}$ occurs for the largest $\frac{L}{D}$. McKinley[3] has also concluded that to obtain minimum energy dissipation in the performance of a mission requires the largest possible $\frac{L}{D}$. This conclusion was based on stress calculations considering axial loads only.

However, the effect of hydrostatic head of liquid propellant in the vertical containers modifies this conclusion and intermediate values of $\frac{L}{D}$ are in fact the most efficient. This is shown in Fig. 2 based on calculations by Sechler[4]. Also, preliminary calculations considering lateral loads, and the problems of structural stiffness, support this view.

3. Axial (e.g. Thrust) Loads

The design case in which the axial thrust of the motor is reacted by drag and inertia forces along the vehicle axis, is probably the most critical for the launching vehicle. Unfortunately, the elastic buckling of thin walled circular cylinders under axial compression shows considerable disparity between theory and experiment. In fact the classical small deflection theory considerably overestimates the critical stress.

Theoretical studies using large deflection elastic deformation equations, and allowing for initial imperfections of the cylindrical shell, have now been made and good agreement obtained with experiment. However, for design purposes the theoretical treatment is inadequate and the problem must be considered on an empirical and statistical basis. This is particularly so when the problem of combined axial compression and internal pressure is considered.

4. Combined Axial Compression and Internal Pressure: Unstiffened Cylinders

The requirement that large volumes of propellant be contained under pressure and the simultaneous transmission of vehicle loads has led to the establishment of thin pressurised cylindrical shells as dominant structural forms for space launching vehicles.

It is believed that the designers in this country use similar information to that given in the R.Ae.S. Data Sheet 04.01.01. (Fig. 3) where if the critical stress is expressed by

$$\sigma_{crit} = KE\frac{t}{R} \quad , \qquad (4.1)$$

the buckling stress coefficient K is plotted against the initial eccentricity parameter δ/t for various values of the pressure parameter, $\frac{p}{E}\left(\frac{R}{t}\right)^2$. The initial irregularity or eccentricity, δ, is believed to play an important part in the prediction of the critical stress for circular cylinders under axial compression and the results shown in Fig. 3 have been obtained from a large number of experiments and show the dependence of δ/t on R/t.

There have also been several admirable summaries in the U.S.A. on this same topic, notably by Gerard[5] and Klein[6], but in spite of a vast amount of theoretical and experimental work carried out throughout the world, simple design curves are still not universally agreed. Work at the College of Aeronautics on these topics has

continued for some time both from a theoretical[7, 8] and experimental[9] point of view. Figs. 4-6 show buckled forms of unstiffened cylinders under combinations of loading of axial compression, internal pressure and torsion. Fig. 7 shows the corresponding instability interaction curve obtained from this series of tests.

The use of results such as these for pressurised aircraft has shown that the fuselage buckling stress is increased during flight due to fuselage pressurisation. For ballistic missiles and space vehicles however, the philosophy of pressure stabilisation is rather different, in that a sufficiently high internal gas pressure is introduced so that the longitudinal tensile stress due to the pressure approximately equals the maximum compressive stress which has to be carried, principally from the axial thrust loads.

Although the compressive buckling stress is increased by the use of internal pressure it can be shown that there is little weight penalty in typical space structures, in designing a pure monocoque structure, to preclude the possibility of any net axial compressive stresses.

Another effect of the internal pressure is to cause circumferential tensile stresses in the structure and similar stresses are caused by axial compressive loads and hydrostatic heads of liquid. Thus there is a limit to the extent of internal gas pressurisation which is permissible. In aircraft pressure cabin design the hoop stress is generally limited by the consideration of crack propagation and there is no reason why a similar criterion could not be used in the design of a launching vehicle. If crack propagation characteristics are not critical the limiting hoop stress could be much higher but should not exceed the material yield stress.

An analysis of an unstiffened cylindrical shell subjected to axial compression, internal gas pressure and hydrostatic pressure has been made[8] and Fig. 8 shows the loading system considered.

For this combination of loads in a vertical circular shell a simple equation for the axisymmetric radial deformation of the shell is

$$D\frac{d^4w}{dx^4} + \frac{Et}{R^2}w = Z \qquad (4.2)$$

where Z, the effective lateral pressure is given by

$$Z = p\left(1 - \frac{\nu}{2}\right) + N\rho_i(\ell - x) + \frac{F\nu}{2\pi R^2} \qquad (4.3)$$

Using these equations an approximate expression for the maximum hoop stress in the shell is,

$$\frac{\sigma_{max}}{E} = 1.09\,\frac{R}{t}\,\psi - 2.15\,K\frac{t}{R} \qquad (4.4)$$

where $\psi = \frac{N\rho_i\ell}{E} + \frac{\lambda}{E}$, and $\lambda = \frac{F}{\pi R^2}$ is the structural index in compression.

Using the most critical uppermost line BB in the R.Ae.S. data sheet (Fig. 3) to obtain K, and the limiting hoop stress criterion, Fig. 9 shows the structural efficiency of a pressure stabilised shell compared with an unpressurised shell having

the same material properties viz.

$$E = 28 \times 10^6 \ \text{lb/in}^2 = \text{Youngs Modulus}$$

$$\omega/t = 0.273 \ \text{lb/in}^3 = \text{Density}$$

$$\sigma_a = 170{,}000 \ \text{lb/in}^2 = \text{Allowable Hoop Stress}$$

In Fig. 9 no account is taken of hydrostatic head of liquid and α the weight parameter is given by $\alpha = \omega/R$.

The full line shown is in accordance with R.Ae.S. data sheet 04.01.01. but the dotted line shows the effect of assuming K = 0, i.e. the pressure to be such that no compressive stresses are caused in the shell. Comparison of the solid and dotted curves for the pressurised shell shows that for values of the parameters $\alpha < 2 \times 10^{-4}$ or $\frac{R}{t} > 1500$, or $\lambda < 150$, the assumption K = 0 gives negligible error. It is also concluded from the figure that for low values of the structural index the pressure stabilised shell has a significant weight advantage. This result was previously noted by Sandorff[10]. It can also be shown that for high values of the structural index, conventional stiffening, e.g. axial stringers, is optional in terms of structural efficiency.

The above results prompted an investigation into the effect of the parameter δ/t and hence K on the structural efficiency for various values of the parameter ψ. The results are shown in Fig. 10 for values of $\frac{\delta}{t} = 0$ (K = 0.6 - the classical result) and K = 0 ($\frac{\delta}{t} \to \infty$). The value K = 0 corresponds to full pressure stabilisation, i.e. no net compressive stresses. The difference between the corresponding curves for the extreme values K = 0 and K = 0.6 decreases as $\frac{R}{t}$ increases. This implies that the effect of initial irregularities decreases as $\frac{R}{t}$ increases.

The loading actions considered in the above analysis are typical of a launching vehicle fuel tank and might refer to either tank A or tank B in the schematic drawing shown of a launch vehicle (Fig. 11). Examination of the time dependence of the parameters such as longitudinal acceleration (N) head of liquid (ℓ) and axial compression force F, has been made[11] assuming a constant thrust, constant burning rate motor, and neglecting drag. The axial loading term can be expressed quite generally as

$$F = N_o \bar{W}_s Z_1 + N_o \bar{\bar{W}}_{so} Z_2 , \qquad (4.5)$$

where $\bar{W}_s$ is independent of time and $\bar{\bar{W}}_{so}$ is the initial value of $\bar{\bar{W}}_s$ which is linearly dependent on time. The hydrostatic fuel loading can be written as

$$\rho_i N \ell = \rho_i N_o \ell_o . Z_2 . \qquad (4.6)$$

The parameters Z_1 and Z_2 have the following dependence on time (T) (Fig. 12)

$$Z_1 = 1 \Big/ \left[1 - \frac{W_p}{W_o} \frac{T}{T_F} \right] \quad \text{and} \quad Z_2 = \left[1 - \frac{T}{T_F} \right] \Big/ \left[1 - \frac{W_p}{W_o} . \frac{T}{T_F} \right] .$$

The analysis suggested that tank A, the upper tank, has its maximum compressive loads at burnout when the hoop stresses due to hydrostatic head are low.

For tank B however the worst axial loading case is at launch when the hydrostatic head is also a maximum. Assuming the launching vehicle of Fig. 11 to weigh 300,000 lb. of which 90 per cent consists of fuel and oxidant,and making similar assumptions to those above, then Fig. 13 shows the effect of axial loads due to longitudinal acceleration.

5. Pure Monocoque versus Semi-Monocoque Construction (Ref. 2)

Propellant tanks are often made of pressurised monocoque construction whereas interstage structure is usually semi-monocoque, axially stiffened structure because it cannot easily be pressurised. This latter form has many advantages for propellant tanks also; especially if they are partly pressurised. It provides for continuity of structure at an intersection of tank wall and interstage structure whereas a mixture of the two types of construction leads to load diffusion problems and the requirement for special reinforcing rings to facilitate the diffusion of concentrated loads e.g. thrust and control loads, into the pure monocoque cylinder.

Crack propagation problems can be minimised by the presence of axial stiffeners and rings which act as crack stoppers. Axial stiffeners may be essential in the lower stages and tanks of a launching vehicle if there is a requirement for the upper stages and tanks to be full when the lower ones are unpressurised.

It is worth noting that the first ballistic missile relying on internal pressure for structural integrity was the MX-774 (Fig. 14). Actually it only needed the strength provided by internal pressure to resist flight loads as it could stand erect on the ground without pressure even when fully loaded. In the Atlas however pressure stabilisation is used to the full. Fig. 15 shows the completed 60 ft. Atlas shell being moved by cranes; all external supports have been removed from the thin walled tanks and only pressurisation enables it to maintain its shape. In contrast Fig. 16 shows the heavily wrinkled skins of the missile during construction.

6. Lateral Loads[10]

An important design load problem for earth take-off vehicles is the complex one involving aerodynamic disturbance due to lateral winds acting on the ascending vehicle and the dynamic response of the vehicle and its control system. A typical design condition is shown in Fig. 17 and it is in the altitude range of 30,000 to 40,000 ft. that a typical space launching vehicle would experience its maximum dynamic pressure at a speed of about 2000 ft/sec.

The resultant structural loads on encountering these lateral wind conditions depend on the guidance philosophy adopted. Programmed attitude results in substantial loads, and control with respect only to angle of attack yields minimum loads but considerable trajectory displacement. A useful reference on this topic is that of Geissler[12].

In space, only manoeuvring and control conditions produce external lateral loads of any magnitude and the time scale can be of such an extent that the loads are very small.

The bending moments and shear forces caused by the lateral loads must be considered in the design of the structure. It has been shown approximately that the stability of an unstiffened cylindrical shell under an applied bending stress distribution may be deduced from the known behaviour of the shell in compression since the maximum bending stress dictates the shell's stability.

If one reconsiders the analysis of an unstiffened shell subjected to internal pressure and axial compression, and an external longitudinal bending moment M is also applied to the shell, then for the case K = 0 the results of Fig. 10 still apply where the parameter ψ is now defined as

$$\psi' = \frac{N\rho_i \ell}{E} + \frac{\lambda}{E} + \frac{2M}{\pi R^3 E} \quad . \tag{6.1}$$

7. Thermal Effects

In unstiffened circular cylindrical shells thermal stresses can arise from radial, circumferential, or axial temperature gradients, and discontinuity stresses can also occur at the junction of the shell with any other member having different thermal expansion properties and/or temperature distributions.

Radial gradients should not be a problem in the class of thin shells considered in this paper but circumferential and axial gradients give rise respectively to axial and circumferential stress distributions which may be significant.

Considerable attention has been given in recent years to the problem of the buckling of cylindrical shells due to thermal stress and this will now be considered for shells subjected to either non-uniform circumferential or axial temperature distributions. It is assumed that material properties are invariant with temperature.

Re-entry problems will not be considered in this paper but reference is made to a good descriptive paper (Ref. 13) and to a useful design study (Ref. 14).

7.1. Circumferential Temperature Gradients

The thermal buckling of simply supported cylinders due to circumferential temperature variations has been studied by Abir and Nardo (Ref. 15). The main conclusion reached was similar to that found for cylinders subjected to a longitudinal bending moment viz. the critical axial thermal stress under a variable circumferential thermal stress distribution is close to the critical axial stress of the cylinder under uniform axial compression.

7.2. Axial Temperature Gradients

Hoff[16] and Johns et al[17] have considered the circumferential buckling of circular cylinders subjected to a uniform temperature rise where the discontinuity stresses are the cause of buckling. The analyses were for simply supported and clamped edges, respectively, and for a uniform shell temperature rise T_c and a rigid non-expanding bulkhead, the corresponding expressions for the circumferential thermal stresses are

$$\sigma_\phi = -E\alpha_c T_c e^{-\mu x}\cos\mu x \ \ldots \text{ (simply supported edges)} \tag{7.1}$$

$$\sigma_\phi = -E\alpha_c T_c e^{-\mu x}(\cos\mu x + \sin\mu x) \ \ldots \text{ (Clamped edges)} \tag{7.2}$$

These stresses are caused by the restraint of the bulkhead and they decay rapidly as distance from the bulkhead is increased, as shown in Fig. 18. Thus local buckling near the joint may occur.

For an axi-symmetric axial temperature distribution the resultant equation to be solved for the shell radial deflection is

$$\frac{d^4w}{dx^4} + 4\mu^4 w = 4\mu^4 . \alpha_c R T_{(x)} \tag{7.3}$$

If $T_{(x)}$ can be approximated as $T_{(x)} = \sum_{m=0}^{3} F_m x^m$ the above equation can be solved for a semi-infinite shell to give

$$w = e^{-\mu x} \left[C_1 \sin\mu x + C_2 \cos\mu x \right] + \alpha_c R T_{(x)}. \tag{7.4}$$

The constants C_1 and C_2 are determined from the shell edge boundary conditions. For a shell attached to a rigid non-expanding frame or bulkhead the appropriate equations 7.1 and 7.2 may be obtained if the shell temperature rise is uniform.

The buckling solution is based on Donnell's uncoupled equilibrium equation for the radial displacement w and an infinite series is used to represent the axial distribution of the circumferential stresses. The radial displacement is also expressed in terms of a Fourier series which satisfies the edge boundary conditions, but not, in general, the equilibrium equation. An approximate solution is then obtained by applying the Galerkin operation, and an infinite set of homogenous linear equations is formulated involving unknown deflection coefficients. The criterion for buckling is that the determinant formed by the multiplying factors of the deflection coefficients should be zero.

Analyses of this type in the past (e.g. Ref. 16) have required a large number of terms in the Fourier series representing the stress distribution over the length of the shell in order to achieve satisfactory representation. However, for the type of buckling considered the length of the cylinder L in the analysis, may be taken as the length near to each end over which the compressive hoop stresses are present. This length is referred to as the 'buckled length' L. This concept has the advantage that only a few terms are required in the Fourier series to accurately represent the circumferential stresses near the ends of the cylinder. From analyses made at the College of Aeronautics (Ref. 17) the variation of buckling temperature rise $(\alpha_c T_c)_{crit}$ as a function of R/t has been determined (Fig. 19) for both simply supported and clamped cylinders subjected to uniform shell temperature rise. In practice of course this uniformity cannot be achieved and in Ref. 17 further analyses have been made in which experimentally measured axial temperature distributions were used. The correlation of this particular experiment with theory is shown in Fig. 19. The experimental details were

$R = 7''$ $\qquad L = 3.5''$

$t = 0.00275''$

$\frac{R}{t} = 2540$

$(T_c)_{crit} = 230^{\circ}C$ - uniform

If $T_{(x)} = \overline{T}\left[0.467 + 1.167x - 0.667x^2\right]$ is the measured distribution

$\overline{T}_{crit} = 324^{\circ}C$, which is the shell centreline temperature

Fig. 20 shows a photograph of the buckle patterns. Calculations show that a combination of axial compression and this mode of buckling should not be critical but it is expected that a combination of torsion with this mode of buckling might be more critical.

8. Dynamic Effects

8.1. Thrust Variations

Hydrostatic pressure levels may be raised significantly by dynamic effects arising from longitudinal thrust variations and the symmetrical surging associated with fluid compressibility and tank wall elasticity. An overload factor approaching 2 is possible especially if the time for acceleration to build up is less than the period of the surging mode. The undamped natural period for the dynamic system in a simple cylindrical tank is approximately

$$T_{n\ surge} = 2\pi\sqrt{\frac{2}{3}\ell^2\,\rho_i\left(\frac{R}{tE} + \frac{1}{2K_i}\right)} \qquad (8.1)$$

K_i = liquid bulk modulus.

8.2. Fuel Sloshing[10]

The interaction of propellant sloshing with engine thrust vectoring is a distinct possibility and coupling with vehicle bending and control dynamics is also likely. The natural frequency of the side-to-side sloshing of fluid in circular cylindrical tanks with the free surface more than one diameter above the bottom may be roughly predicted by the formula

$$f_{n\ slosh} = 1.7\sqrt{N/D} \qquad (8.2)$$

N = accel. (g's)

D = tank dia. (ft.)

Sloshing raises the natural frequency and effective damping of the structural modes but the control of sloshing would be easier if the frequency of the vehicle autopilot system could be made low compared with that of the lowest sloshing mode. Sloshing frequencies vary over a range which approaches and may bracket the value that other considerations dictate for the autopilot system. However sloshing frequencies vary approximately as $1/\sqrt{D}$ whereas the required autopilot frequency should vary as $1/L^2$. Consequently dynamic interaction should be reduced as the two frequencies diverge in very large vehicles. Unfortunately a decrease in propellant density, e.g. a change to liquid hydrogen, raises the required autopilot frequency.

Note,

$$f_{control} \propto 1/\rho_i L^2$$

$$f_{vehicle} \propto D/L^2 \qquad (8.3)$$

$$f_{slosh} \propto 1/\sqrt{D}$$

8.3 Structural Oscillations

Control system dynamical response is limited also by structural vibratory modes which the gyro and accelerometer sensors confuse with rigid body motion. To avoid coupling effects which may result in saturation or instability various cures have been suggested, e.g.

(a) siting the gyros near an antinode of the troublesome mode (or the accelerometers near a node).

(b) increase damping of lower modes by phase shifting of the thrust response.

(c) stiffening the structure to raise the frequencies of the troublesome modes.

(d) using a slower acting control system.

Methods (a) and (b) appear to have the greatest promise.

8.4. Panel Flutter

8.4.1. Introduction

The term 'flutter' applies to the dynamic instability of an elastic body in an airstream and among its many manifestations e.g. wing flutter, tab flutter, is the phenomenon known as 'Panel Flutter'. This refers generally to the flutter of a thin plate, shell or membrane, one of whose surfaces is exposed to an airstream and the other to still air.

In defining the phenomenon no extraneous excitation which is essentially independent of the motion of the panel needs to be considered, whether it be mechanical or aerodynamic in origin, or regular or random in nature. Thus oscillations caused by aerodynamic noise or turbulence in the flow are not regarded as panel flutter.

That panel flutter may occur at low flow speed is exemplified by the flutter of a flag, but in aeronautical design it seems to be important only in supersonic flight. The corresponding static problem known as panel divergence can occur subsonically but is less important and will not be considered further.

It should be noted that large amplitude panel flutter is likely to occur only for buckled panels (aerodynamic heating may be the cause of buckling); therefore the apparent importance of panel flutter lies in its effect on the structural behaviour particularly the fatigue life.

The influence of thermal stresses and buckling on panels has been shown in tests reported by the N.A.S.A.[18]. In a typical tunnel run at M = 3 with a stagnation temperature of 500°F, a dynamic pressure of 3100 p.s.f. and zero pressure differential on the panel, the panel temperature obviously increased with time. It did not flutter until the temperature reached 150°F and then stopped at 300°F. A theoretical calculation showed that as the panel is heated the compressive thermal stresses increase the susceptibility to flutter. After buckling the additional temperature rise increased the depth of the buckles thereby stiffening the panel and finally stopping the flutter.

The same reference (Ref. 18) also records that panel flutter has been experienced on the corrugation-stiffened curved wing fairings of the X-15. The phenomenon has also been suggested as the cause of structural failure of some of the early German V.2 vehicles.

The problem of panel flutter has received theoretical and experimental investigations at the College of Aeronautics and Fig. 21 shows a flutter model wedge mounted in the working section of the College's 9"x 9" continuous return flow supersonic tunnel. Fig. 22 gives another view showing the clamped edged plate of 6" dia. under investigation.

8.4.2. Cylindrical Panel Flutter: Discussion

Investigations into panel flutter of cylindrical shells with the wind direction along the cylinder axis fall into two distinct categories; relating to unstiffened infinitely long cylinders and cylinders stiffened by rings and longerons.

The former problem has been examined by Miles (Ref. 19) and Leonard and Hedgepeth (Ref. 20), and although the analyses were quite dissimilar the conclusion was reached that infinite cylinders are extremely susceptible to panel flutter. Both analyses assumed travelling wave motions.

The latter problem has received considerable attention in recent years. A full review of these analyses would be out of place here but in a recent paper by the author (Ref. 21) a limited review was made and it was found that the differences between various published analyses and the consequent inconsistencies in the results obtained could be attributed mainly to the assumptions made in the equations of elastic deformation used. A simplified panel flutter analysis is given in an Appendix to this paper.

In the author's view the following effects still need enlightenment. Should the tangential inertia effect be included in the analysis and what are the most appropriate set of elastic equations for this problem ? How does the critical flutter speed depend upon the number of circumferential and axial waves in the flutter mode, and are the trigonometric modes assumed in the analyses truly representative of the shell deformations and edge boundary conditions ?

The author feels that tangential effects should be included and that the elastic equations used should be reasonably exact e.g. Flugge's. Structural damping effects should be considered, especially since it has been shown (Ref. 22) that such effects may be destabilising. The degree of instability in the various critical modes must be assessed and the influence of boundary layer effects on the degree of instability must be verified.

Fig. 23 shows critical thickness/radius ratios for axisymmetric flutter[23]. The extreme conservatism of the travelling wave analyses should be noted. It is also suggested that the standing wave analyses may be unduly conservative in that they neglect aerodynamic damping terms. This is valid for flat plate analyses when structural damping is zero[22] but may not be so for cylindrical shells. Results of analyses into this aspect are given in the Appendix 1.

Fig. 24 shows critical thickness/radius ratios for modes involving circumferential waves i.e. $n \neq 0$, again for an empty steel cylinder with the front edge clamped and the rear edge simply supported. The less critical nature of the results for $n \neq 0$ compared with $n = 0$ suggests that axisymmetric modes are more critical. However it may be that the degree of instability is greater in the $n \neq 0$ case.

It is believed that these latter results may be conservative because the analyses assumed aerodynamic damping effects to be negligible.

9. Environmental Effects in Space

The ultra hard vacuum which applies above a thousand mile altitude cannot at present be duplicated on earth. From such experiments as can be made it is known that surface properties of materials including crack propagation and fatigue characteristics may be strongly affected by vacuum. These properties are particularly significant in the design of thin pressurised shells and may govern structural weight and reliability.

Ionising radiation chiefly of solar origin will have a detrimental effect on the stability of structural and other properties of plastics and organic materials. An interesting review of these and similar problems is given by Reiffel[24].

Damage by meteoritic particles constitutes a major environmental hazard and it has received considerable attention with regard to identification of the environment, nature of the damage process and protective design. The results of these investigations are still rather nebulous and Gazley and Bjork[25] have summarised the present situation rather nicely: - "The probability of damage to Space Vehicles ... has appreciable uncertainty because of the difficulty of estimating meteoroid mass and frequency. The results indicate for example that a surface 1 metre square and 1 mm thick will be punctured somewhere between 7 weeks and 620 years".

Fig. 25 taken from Ref. 26 gives estimated thicknesses of various structural materials required for reasonably safe design for a vehicle having an external surface area of 100 ft^2. It is evident that materials having a high elastic modulus are the most efficient for a given thickness but for a given weight beryllium would be superior to stainless steel or molybdenum because of its superior ratio of E/density.

Possible wall constructions for protection against meteoroids are shown in Fig. 26. Fig. 26(a) shows a two (or multi) layer form of construction attributed to Whipple in which the outer layer provides the major heat and meteoroid protection. The inner layer is the main structural shell which also serves as the pressurised cabin wall. If the outer layer were punctured by a meteoroid the resulting fragments should impinge on the inner wall over a wider area than that of the original puncture. This should make penetration of the inner wall unlikely.

The apparently high efficiency of beryllium as a meteoroid shell suggests the use of thin sheets or foils of beryllium placed between the heat shield and cabin wall whenever the heat shield is inadequate for meteoroid protection[13]. Such sheets could also help to minimise internal heat radiation and convection from the heat shield, Fig. 26(b).

Schemes for automatically detecting and sealing a puncture once it occurs should be perfected. The pressurised cabin shell should be constructed of materials having a high resistance to catastrophic bursting in the presence of a crack or hole.

10. Ground Loads

The problems of handling and transporting the large structures required for space missions will require special treatment. One approach of course is to use clusters of smaller tanks rather than large tanks in each stage of the vehicle - but there is an associated weight penalty. The use of structures employing full pressure stabilisation will require special non-flight supporting structure during these phases - or else the full internal pressurisation - to maintain structural shape and rigidity. This was evidenced by the two figures of the Atlas missile.

Loads occurring on the launch pad when the vehicle is vertical include those due to wind shears and horizontal gusts, which are particularly important when the vehicle is supported only at its base and the shelter of the servicing tower is removed.

In addition there is then a possibility that the slender structure might be excited by Von Karman vortices, a phenomenon that has been observed on many occasions and is widely reported in the literature[27, 28]. For a certain range of Reynolds No. (based on cylinder diameter) - approximately $10^2 < R_n < 5 \times 10^5$ vortices are shed alternately from opposite sides of the cylinder causing an oscillating force perpendicular to the airstream and cylinder axis. The frequency (f) of vortex shedding is expressed in terms of the airstream velocity (U) and cylinder diameter by the Strouhal No. $k = \frac{fD}{U}$. Fig. 27 shows the variation of k with Reynolds No. In general oscillations occur when the eddy frequency (f/cycles/sec) coincides with the natural frequency of the cylinder, and whether or not such oscillations occur in the range of wind velocities of interest depends upon the natural frequency, the amount of damping in the structure, and its precise cross-sectional shape. The influence of damping for a circular cylinder is shown also in Fig. 27.

The significance of this phenomenon is that it may induce the low frequency cantilever bending modes and may lead to a fatigue condition. If the problem is critical a possible cure is to use external stiffeners which act as spoilers.

11. Impact Loads[13]

Recovery of the re-entry vehicle may be accomplished by means of a drag chute, or by a retro-rocket decelerated landing, for ballistic entry types, and a more or less conventional type of landing for glide vehicles. Ballistic vehicles will experience high impact loadings particularly for ground impact. The shock transmission to the occupants can possibly be reduced by designing a sufficient length of collapsible shell structure forward of the occupant mounting point, with the proviso that for a water landing, leakage of water into the cabin be precluded.

Fig. 28 shows the rigid body decelerations of a blunt nosed vehicle, impacting vertically on water with an initial velocity of 50 f.p.s., versus the penetration depth ratio d/h_o. The deceleration pulse rises to a peak value of 23g and falls below 5g in a total elapsed time of slightly greater than .1 sec. In addition the rate of increase of deceleration to the peak value of 23g is less than 800g per sec. Human tolerance to shock loading depends apparently on the combination of peak g and rate of rise to peak. In this respect the best body position is supine with the maximum distribution of deceleration forces over the rear portions of the body. Shock tests have shown that a rate of rise of 1000 g/sec., to a peak of 30g is tolerable, whereas a rate of 1500g/sec. to a peak of 40g results in unconsciousness[29].

Both peak g and rate of rise depend on the frontal shape of the impacting body. The greater flatness the higher is the deceleration peak and the rate of rise.

12. Inflatable Space and Re-Entry Vehicles

One interesting suggestion for possible space applications and for achieving manned re-entry from orbital flight is the inflatable glider.

The present state of the material art is such that materials to resist the anticipated maximum temperatures of 1500°F are not now available 'off the shelf' although development work is in progress.

Fig. 29 shows a typical example of an inflated re-entry vehicle[30] and the two basic types of structural elements represented. The inflated circular cylinder typifies the fuselage construction and the inflated plate is used for wings, fins and control surfaces.

Two possible arrangements of plate construction are also shown in the Fig. 29, (a) An array of tubes - an inflatable equivalent of multiweb construction, (b) two woven covers held a fixed distance apart by a regular array of fibres called 'dropcords'. This arrangement known as 'airmat' permits the inflated wing to be tapered in any desired manner and from bending strength considerations it is more efficient than the tubular array or any similar configuration of the same depth. Airmat was developed by the Goodyear Aircraft Cirp.

Expandable fabric structures for space missions inherently provide the advantages of minimum structural density, maximum volume/weight ratio and unmatched packageability for the launch phase - making possible full-size erection and development in space with minimum launch penalty.

Such structures are being considered for a wide range of space applications - from manned space stations and ultra lightweight solar concentrators to re-entry vehicles. Fig. 30 shows a Goodyear designed inflated space structure with a central solar collector and communications antenna.

Several examples of inflatoplanes are now flying and the concept is well established. In Great Britain an inflated glider has been designed by Mr. F. Kiernan at R.D.E. Cardington. Flight tests on this wing, with a slightly modified control system, have been made by Mr. O. Neumark at Seaton, Devon (19th September, 1960). These tests have been reported in Ref. 31 and Fig. 31 shows the wing in flight.

The design of expandable structures is very similar to that of conventional structures. The problem of stability under axial compressive and bending loads can be considered in the same way as for thin shells. Assuming $K = 0$ the full pressurisation curves shown earlier are applicable to inflated circular cylinders.

13. Specific Design Studies

Fig. 32 shows OUTPOST III a Manned Space Station designed by K. A. Ehricke of Convair Astronautics. The 4 compartment station to be assembled by Centaur or Saturn Vehicles is proposed for selection and training of space crews, and development of life support systems for deep space missions. The design calls for a weight of 50,000 lbs., 10 ft. in diameter and 140 ft. long (exclusive of end radiators), with nuclear electric power. The nearest end is heavily shielded as electromagnetic storm cellar for 4-8 crew during solar flares.

Aeronutronic Div. of Ford Motor Co. has designed a three man orbiting space vehicle utilising a stiffened cylindrical shell of double wall construction with axially corrugated stiffeners between the walls. Skins of the structure could act as shields against cosmic and solar radiations and meteoric impacts. The design is for a structure approximately 15 ft. in length with a 7 ft. inside diameter which incorporates a highly secure area completely shielded from cosmic radiation. Provision is made for a compartmented interior to allow any section punctured by a meteorite to be sealed off. Fig. 33 shows applications of the Aeronutronic double wall structure. Upper-space station; centre-compartmentation; below-winged re-entry configuration.

A recent paper by R. Haviland[32] contains an interesting study for a manned space vehicle in which he determines the vehicle layout from the following considerations:

(1) Access between the ascent-re-entry capsule to the last stage propellant tank is needed.

(2) Considerations of launch safety make it desirable to have the capsule at the forward end of the vehicle.

(3) Since hydrogen (fuel) + oxygen make desirable propellant mixtures (excess propellant can be used directly to provide oxygen for breathing- or water) and the hydrogen tank will be four times the size of the oxygen tank - only the hydrogen tank will be considered as in-space living quarters.

(4) Considerations of vehicle control suggest a desirable arrangement is to surround the hydrogen tank with the liquid oxygen tank. Since this introduces thermal problems - an equivalent effect - providing effective double wall construction is secured by arranging a number of small oxygen tanks around the central hydrogen tank. Haviland suggests internal dimensions of 8 ft. diameter and 20 ft. length for the hydrogen tank to provide a reasonable minimum living and working space. Fig. 34 shows a sketch of the space vehicle's principal features.

Figs. 32 and 34 illustrate the concept that the propellant tanks of the space launching vehicle can be used for the living quarters of a manned vehicle. Because of the considerations of cosmic and solar radiations and meteoric impacts it would appear necessary for such tanks to be of double wall construction, e.g. as in Fig. 33. Thus the use of thin unstiffened cylindrical shell structures would probably be confined to the booster stages only of launching vehicles. Obviously for more complex structures the simplified analyses presented in this paper are not applicable. However the aim of the paper has not been to give practical design guides but to discuss some of the problems of the designer and to relate them to a specific form of construction, viz. the unstiffened shell.

14. Acknowledgement

I would like to acknowledge the assistance given to me, in connection with some of the material presented, by Mr. A. F. Newell.

15. References

1.	Gerard, G.	Structures and materials. Space/Astronautics, vol. 31, March, 1959.
2.	Meissner, C.J.	Some considerations for the preliminary structural design of liquid fuelled boosters. Ballistic Missile and Space Technology, vol. IV, p. 255 (Ed. D. LeGalley) Academic Press, 1960.
3.	McKinley, D.K.	Structure weight and configuration estimating data for very large liquid boosters. ARS Paper 1085-60. Conference on the Structural Design of Space Vehicles, April 1960.
4.	Sechler, E.E.	Structural configurations, analyses and materials for space vehicles. Chap.19 of Space Technology. (Ed. H. Seifert). J. Wiley and Sons (1959).
5.	Gerard, G., Becker, H.	Handbook of structural stability. Parts I - VI. NACA TN. 3781-6. 1957-58.
6.	Klein, B.	Review of design information on buckling of unstiffened thin walled circular cylindrical shells. ARS Journal, vol. 30 No. 1. January, 1960.
7.	Houghton, D.S., Johns, D.J.	Linear buckling of an axially reinforced pressurised cylinder. College of Aeronautics Note No. 110, Oct. 1960.
8.	Houghton, D.S., Johns, D.J.	An analysis of an unstiffened cylindrical shell subjected to internal pressure and axial loading. College of Aeronautics Note No. 114, March, 1961.
9.	Orpe, C.	Buckling of thin circular cylindrical shells. College of Aeronautics Thesis (Unpublished), June, 1961.
10.	Sandorff, P.E.	Structures considerations in design for space boosters. ARS Journal vol. 30, No. 11, November, 1960.
11.	Houghton, D.S., Johns, D.J.	Design problems of ballistic missile tank structures. Aircraft Engineering, vol, 33, July, 1961.
12.	Geissler, E.D.	Problems in a titude stabilisation of large guided missiles. I.A.S. Paper, No. 60-63, June, 1960.

References (Continued)

13.	Coppa, A.P.	Structural considerations of manned space vehicles. ARS Journal, vol.30, No. 1. January, 1960.
14.	Kelly, O.A.	Parametric weight study of a manned space entry vehicle. Aero/Space Engineering, vol.19, No.10, October, 1960.
15.	Abir, D., Nardo, S.V.	Thermal buckling of circular, cylindrical shells under circumferential temperature gradients. Journal Aero/Space Sci.December, 1959.
16.	Hoff, N.J.	Buckling at high temperature. Journal Royal Aeronautical Society, vol.61, No.11, November, 1957.
17.	Johns, D.J., Houghton, D.S., Webber, J.P.	Buckling due to thermal stress of cylindrical shells subjected to axial temperature distributions. College of Aeronautics Report No.147, May,1961.
18.	Kordes, E.E., Tuovila, W.J., Guy, L.D.	Flutter research on skin panels. NASA TN. D.451, September, 1960.
19.	Miles, J.W.	Supersonic panel flutter of a cylindrical shell. Journal Aeronautical Sci. Part I, pp.107-118, 1957, Part II pp.312-316, 1958.
20.	Leonard, R.W., Hedgepeth, J.M.	On panel flutter and divergence of infinitely long unstiffened and ring-stiffened thin walled circular cylinders. NACA Report, 1302, 1957.
21.	Johns, D.J.	Supersonic flutter of cylindrical shells. College of Aeronautics Note No.104, July,1960.
22.	Johns, D.J., Parks, P.C.	Effect of structural damping on panel flutter. Aircraft Engineering, vol.32, October, 1960.
23.	Fung, Y.C.	Panel flutter. AGARD Manual on Aero-Elasticity. November,1959.
24.	Reiffel, L.	Structural damage and other effects of solar plasmas. ARS Journal, vol.30, No.3. March, 1960.
25.	Gazley, C., Bjork, R.L.	Estimated damage to space vehicles by meteoroids. Rand Corp. Res. Memo. RM 2332, February,1955.

References (Continued)

26.	Kornhauser, M.	Estimates of the penetration of the skin of a satellite by meteoroids. General Electric Co. Missile and Space Division Report, April, 1958.
27.	Freese, C.E.	Vibrations of vertical pressure vessels. Trans. A.S.M.E., Series B. February, 1959.
28,	Scruton, C.	Wind excited oscillations of tall stacks. The Engineer, July 10th, 1955.
29.	Stapp, J.P.	Effects of mechanical forces on living tissue. Journal Aviation Medicine, vol.26, No.4, August, 1955.
30.	Leonard, R.W., Brooks, G.W., McComb, H.G.	Structural considerations of inflatable re-entry vehicles. NASA TN. D.457. September, 1960.
31.	Neumark, O.	Inflated wings. Aeroplane, March 23rd, 1961.
32.	Haviland, R.P.	Designing for man in space. Spaceflight, vol.III, No.3, May 1961.

APPENDIX 1.

Cylindrical Panel Flutter: Analysis

The general deformation equations for thin circular cylindrical shells may be written in the general form,

$$\begin{vmatrix} A_{uu} & A_{vu} & A_{wu} \\ A_{uv} & A_{vv} & A_{wv} \\ A_{uw} & A_{vw} & A_{ww} \end{vmatrix} \begin{vmatrix} u \\ v \\ w \end{vmatrix} = \left(\frac{1-\nu^2}{Et}\right) \begin{vmatrix} X \\ Y \\ Z \end{vmatrix} \qquad (A.1)$$

The operators A_{ij} have the general form $B_{ij} + \frac{t^2}{12R^2} C_{ij}$, and for example, according to Novozhilovs equations

$$B_{vv} = \frac{1-\nu}{2} \frac{\partial^2}{\partial x^2} + \frac{1}{R^2} \frac{\partial^2}{\partial \phi^2} ,$$

and

$$C_{vv} = 2(1-\nu) \frac{\partial^2}{\partial x^2} + \frac{1}{R^2} \frac{\partial^2}{\partial \phi^2} .$$

X, Y, Z, are the external loadings on the shell element, and u, v, w are the corresponding displacements assumed to have the forms,

$$\begin{aligned} u &= e^{i\Omega T} \sum U_{mn} \operatorname{cosn}\phi \cos\frac{m\pi x}{L} \\ v &= e^{i\Omega T} \sum V_{mn} \operatorname{sinn}\phi \sin\frac{m\pi x}{L} \\ w &= e^{i\Omega T} \sum W_{mn} \operatorname{cosn}\phi \sin\frac{m\pi x}{L} \end{aligned} \qquad (A.2)$$

If it is assumed that the tangential loadings are zero, i.e. X = Y = 0, equation A.1 can be expanded, using expressions A.2 to give the closed form result for the deflection w

$$w \frac{\Delta_1}{\Delta_2} = \left(\frac{1-\nu^2}{Et}\right) Z \qquad (A.3)$$

where Δ_1 is the determinant formed by the A_{ij} terms in u, v and w, and Δ_2 is the determinant formed by the A_{ij} terms in u and v only. If the aerodynamic forces are expressed by linear piston theory the lateral loading Z is given by

$$Z = -\left[\frac{\rho U^2}{M} \frac{\partial w}{\partial x} + \frac{\rho U}{M} \frac{\partial w}{\partial T} + \omega \frac{\partial^2 w}{\partial T^2} \right] . \qquad (A.4)$$

By applying the Galerkin operation to equation A.3 the resulting flutter determinant may be solved for the flutter frequency, Ω, and speed, U. If axi-symmetric flutter

is assumed, i.e. n = 0, a simple equation for the shell radial deflection mode w is

$$D\frac{d^4w}{dx^4} + \frac{Et}{R^2}w = Z \qquad (A.5)$$

and a two degree of freedom analysis (m = 1, 2) yields the simple flutter criterion (Ref. 1):

$$\Omega^2 = \frac{D}{2\omega}\left[17\left(\frac{\pi}{L}\right)^4 + 8\mu^4\right] \qquad (A.6)$$

$$\frac{256}{9}\left[\frac{\rho U^2}{LM}\right]^2 = 225\frac{D^2\pi^8}{L^8} + 4\left[\frac{\rho U\Omega}{M}\right]^2 \qquad (A.7)$$

It is believed that the neglect of the aerodynamic damping term $\left[\frac{\rho U\Omega}{M}\right]$ in equation A.7 cannot be justified for cylindrical shells, and this is emphasised by the results for a particular shell in Table 1, Axisymmetric flutter was assumed and both Flugge's[2] and Novozhilov's[3,4] equations of equilibrium were used.

References

1. Johns, D.J. — Supersonic flutter of a cylindrical panel in an axisymmetric mode. Journal Royal Aeronautical Society, June, 1960.

2. Flugge, W. — Statik und Dynamik Schalen. Julius Springer, Berlin, 1939.

3. Novozhilov, V.V. — The theory of thin shells. Noordhoff Ltd., 1959.

4. Houghton, D.S., Johns, D.J. — Deformation equations for non-circular cylinders. Journal Royal Aeronautical Society, Dec. 1960.

TABLE 1.

Critical Mach No.
For Light Alloy Cylindrical Shell at Sea Level

$\frac{t}{L} = 6 \times 10^{-3}$, $\frac{L}{R} = 2$, L = 2 ft., n = 0

Elastic Equations	4 Mode Solution m = 1, 2, 3, 4	2 Mode Solution m = 1, 2	2 Mode solution m = 1, 2 No. Aero. Damping
Flugge	9.5	11.2	2.5
Novozhilov	9.6	11.2	2.6

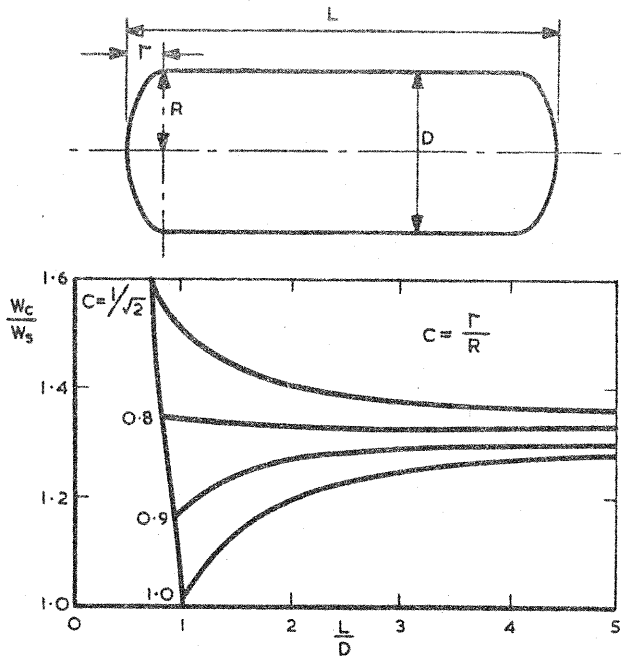

FIG. 1. WEIGHT RATIO OF PRESSURISED CYLINDERS AND SPHERES.

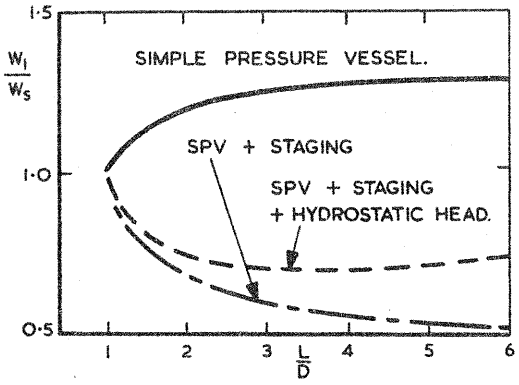

FIG.2.WEIGHT RATIO FOR PRESSURISED, STAGED, CYLINDERS AND SPHERES.

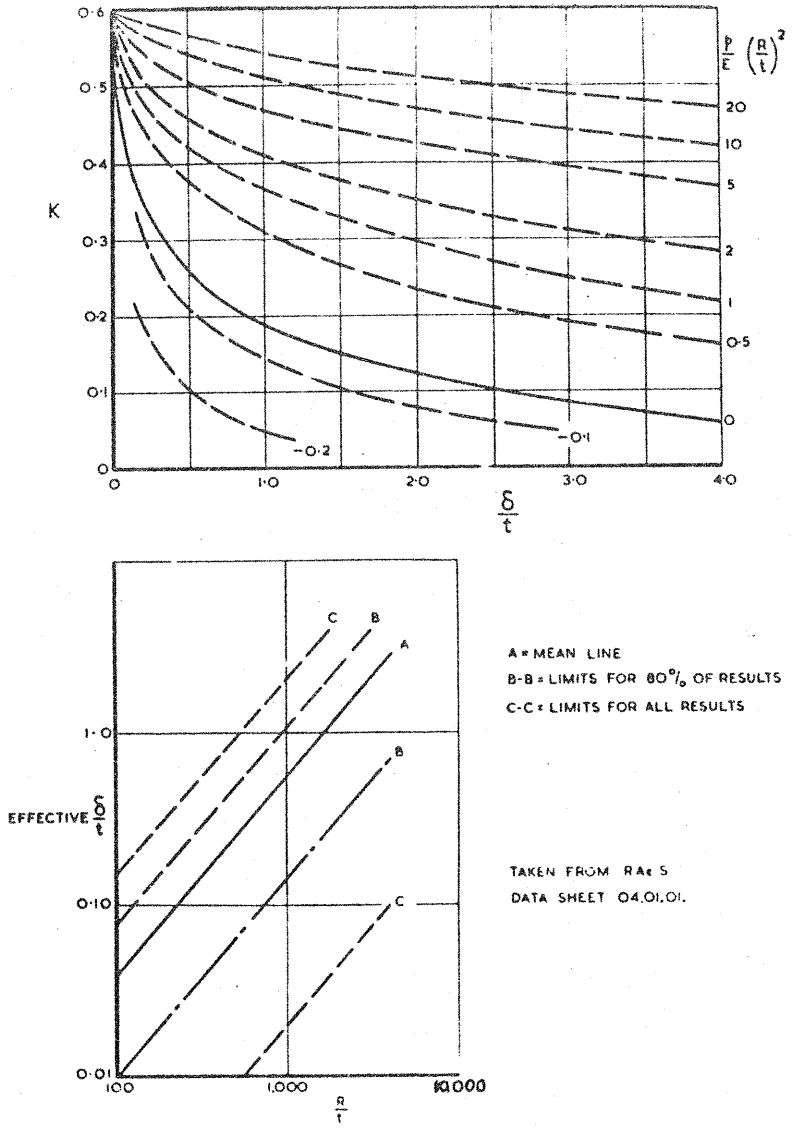

FIG. 3. BUCKLING STRESS COEFFICIENTS FOR THIN WALLED UNSTIFFENED CIRCULAR CYLINDERS UNDER COMBINED AXIAL COMPRESSION AND INTERNAL PRESSURE

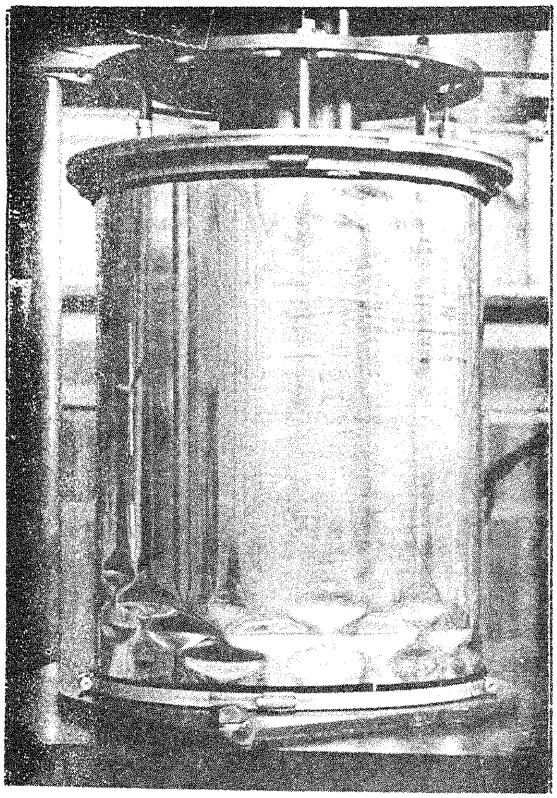

FIG. 4. BUCKLED MODE FOR CYLINDER SUBJECTED TO AXIAL COMPRESSION AND INTERNAL PRESSURE

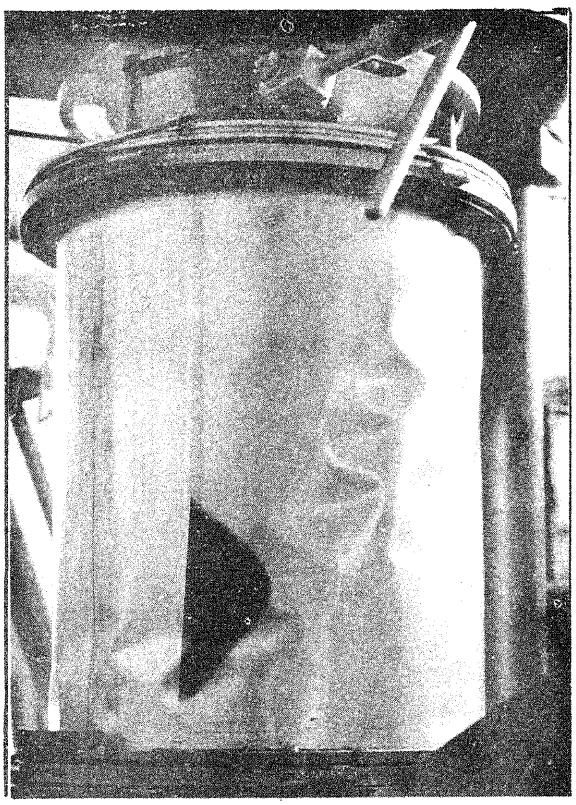

FIG. 5. BUCKLED MODE FOR CYLINDER SUBJECTED TO AXIAL COMPRESSION, INTERNAL PRESSURE AND TORSION

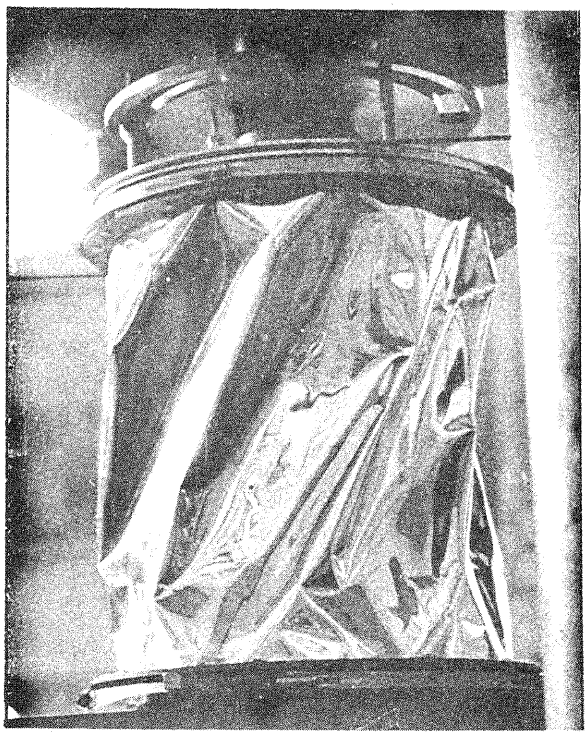

FIG. 6. POST-BUCKLED MODE FOR CYLINDER SUBJECTED TO LARGE TORSION/AXIAL COMPRESSION RATIO, ZERO INTERNAL PRESSURE

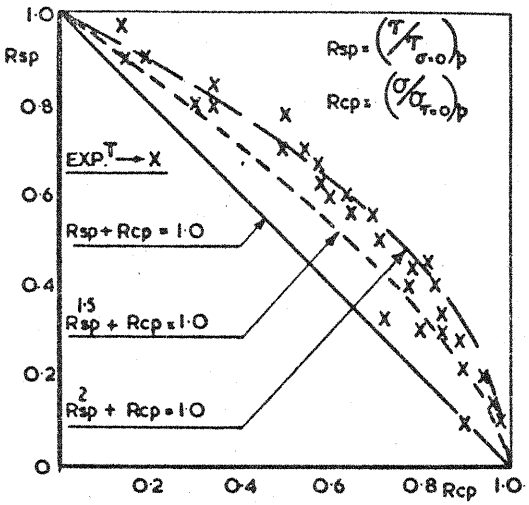

FIG. 7. INTERACTION CURVES FOR CYLINDRICAL SHELL UNDER TORSION AND COMPRESSION. SHELL PARAMETERS: R = 7", t = .01", L = 18" τ = CRITICAL TORSIONAL SHEAR STRESS, σ = CRITICAL COMPRESSIVE STRESS, STRESSES MEASURED AT INTERNAL PRESSURE p

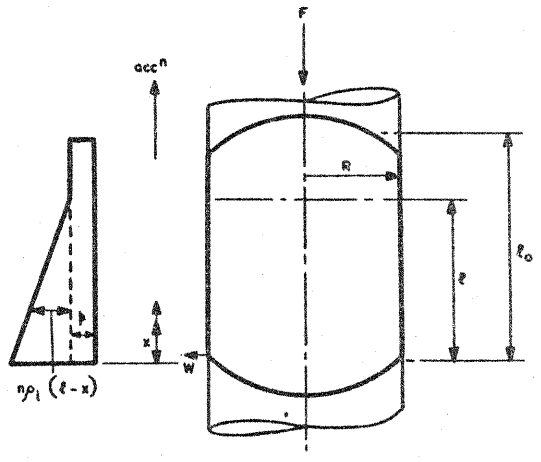

$$\frac{d^4W}{dx^4} + 4\mu^4 W = \frac{1}{D}\left[P\left(1-\frac{\nu}{2}\right) + N\rho_i\left(\ell - x\right) + \frac{F\nu}{2\pi R^2}\right]$$

FIG. 8. FUEL TANK LOADING SYSTEM

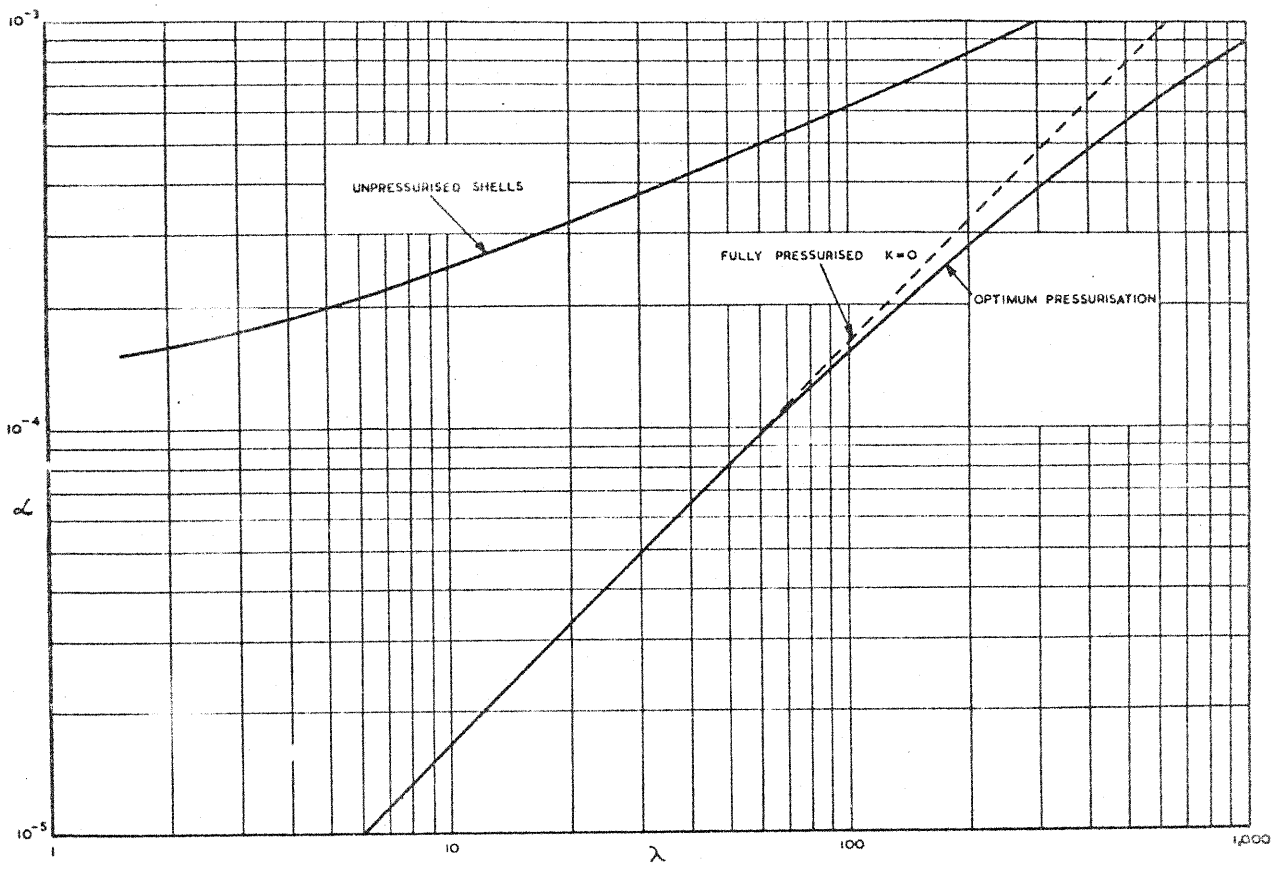

FIG. 9. STRUCTURAL EFFICIENCY OF UNSTIFFENED SHELLS IN COMPRESSION

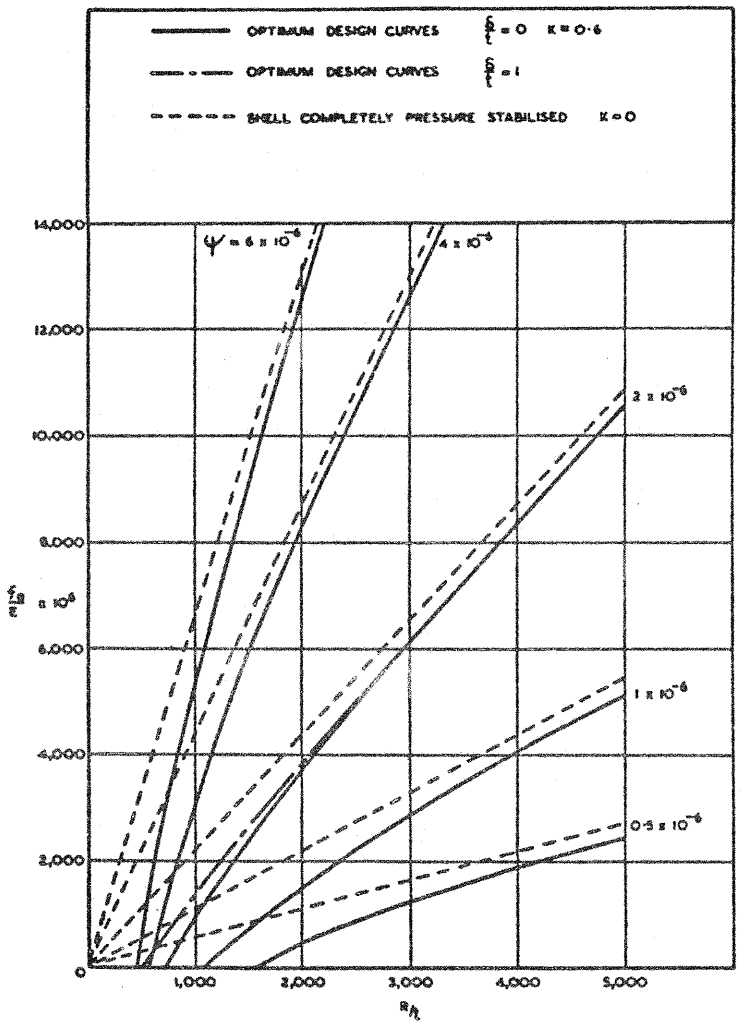

FIG. 10. OPTIMUM SHELL $\frac{R}{t}$ RATIOS FOR FOR GIVEN LOADING ψ AND ALLOWABLE HOOP STRESS σ_a

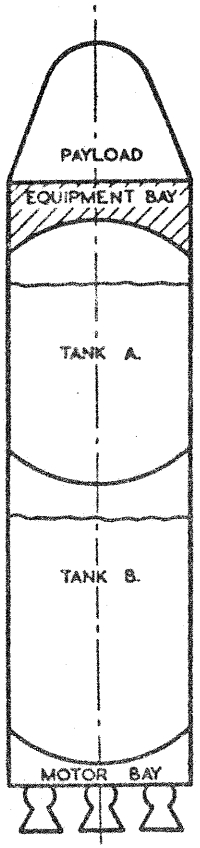

FIG. 11. TYPICAL LAUNCHING VEHICLE CONFIGURATION

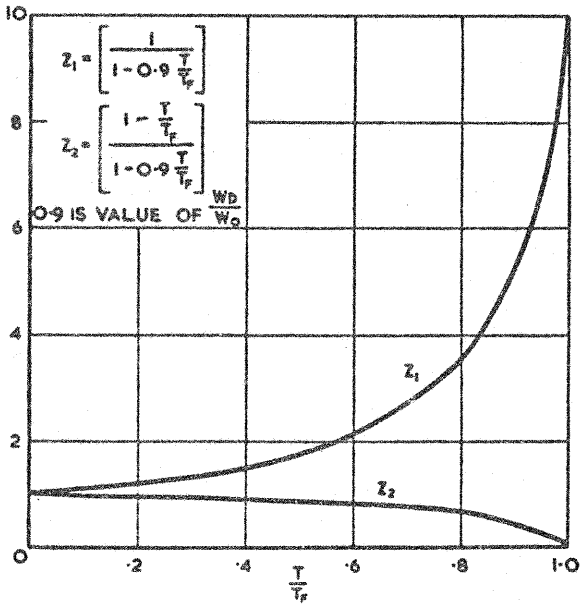

FIG. 12. SHELL LOADING PARAMETERS Z_1, Z_2.

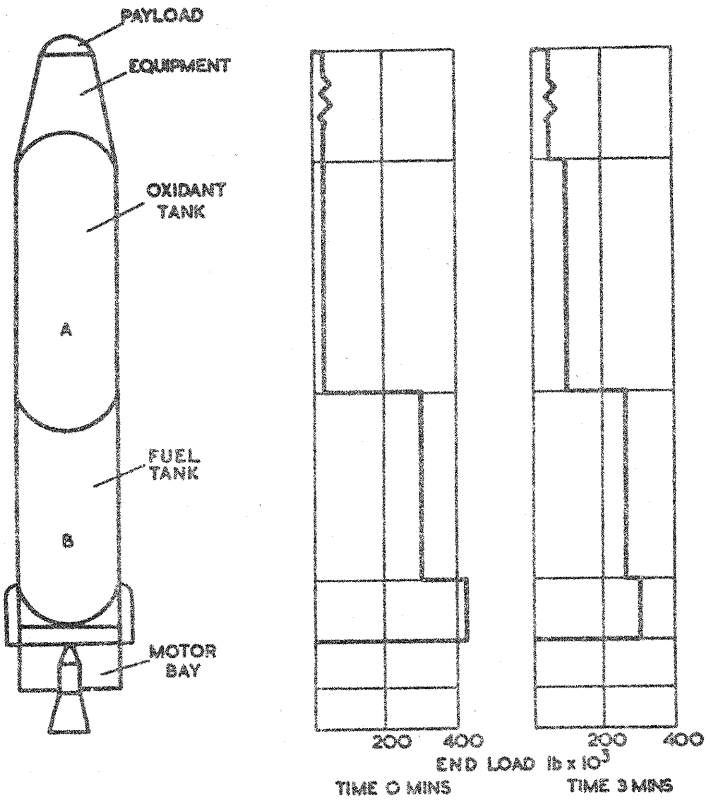

FIG. 13. AXIAL LOADING CASES OF HYPOTHETICAL LAUNCH VEHICLE

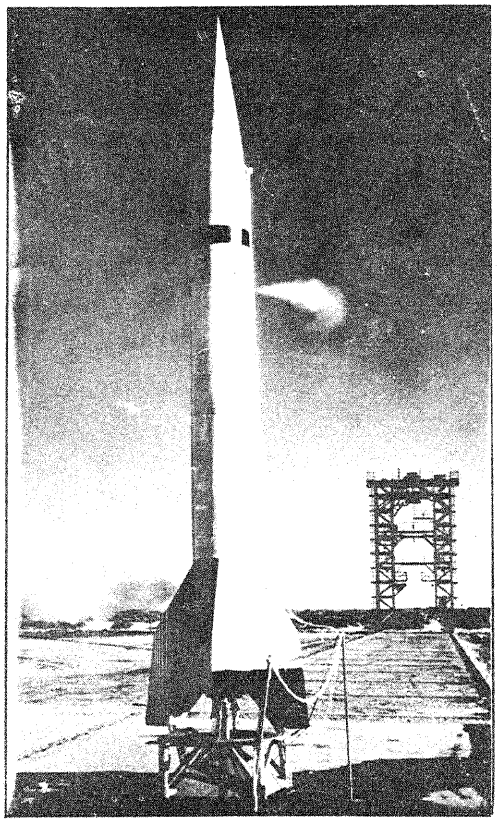

FIG. 14. MX-774. THE FIRST MISSILE RELYING ON INTERNAL PRESSURE FOR STRUCTURAL INTEGRITY

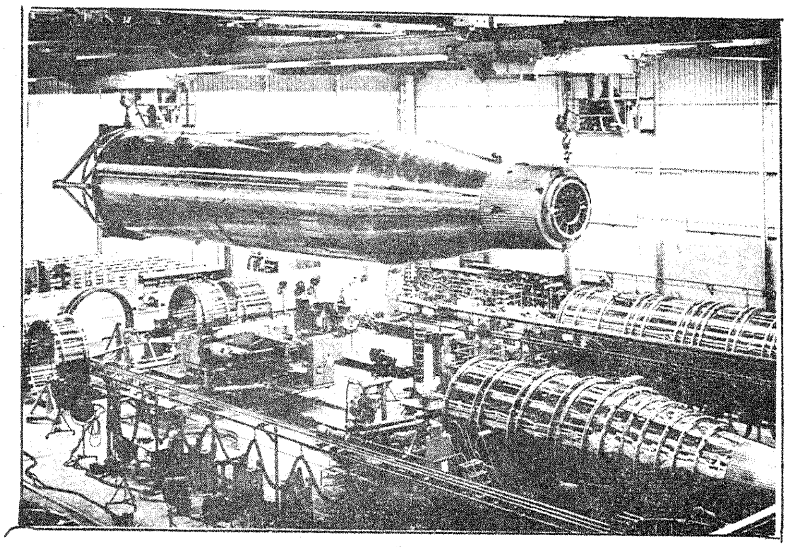

FIG. 15. THE COMPLETED, PRESSURISED, ATLAS SHELL

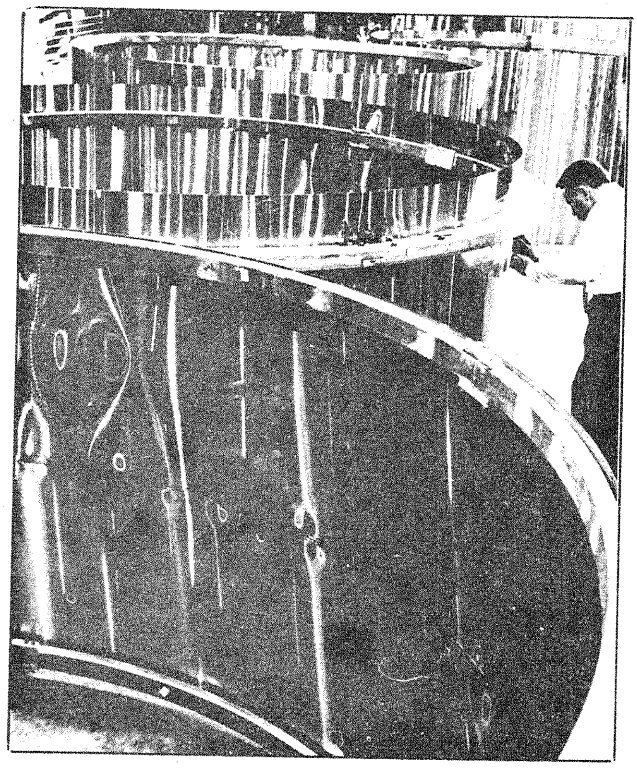

FIG. 16. SECTIONS OF ATLAS SHELL UNDER CONSTRUCTION

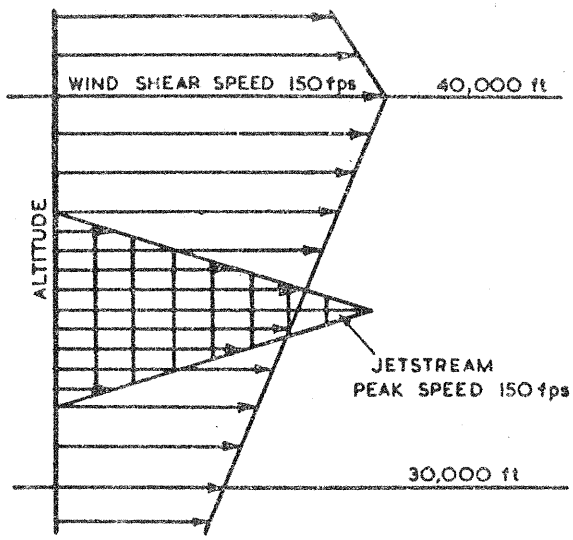

FIG. 17. TYPICAL LATERAL WIND CONDITIONS

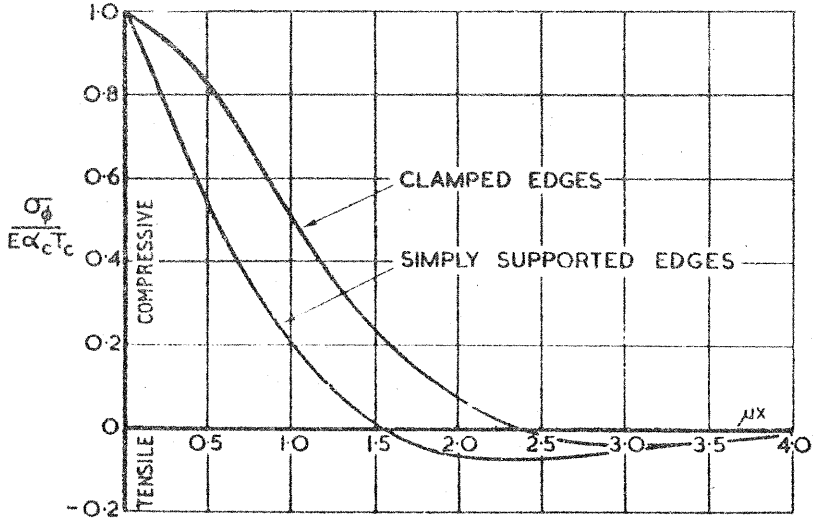

FIG. 18. CIRCUMFERENTIAL THERMAL STRESSES IN CYLINDER

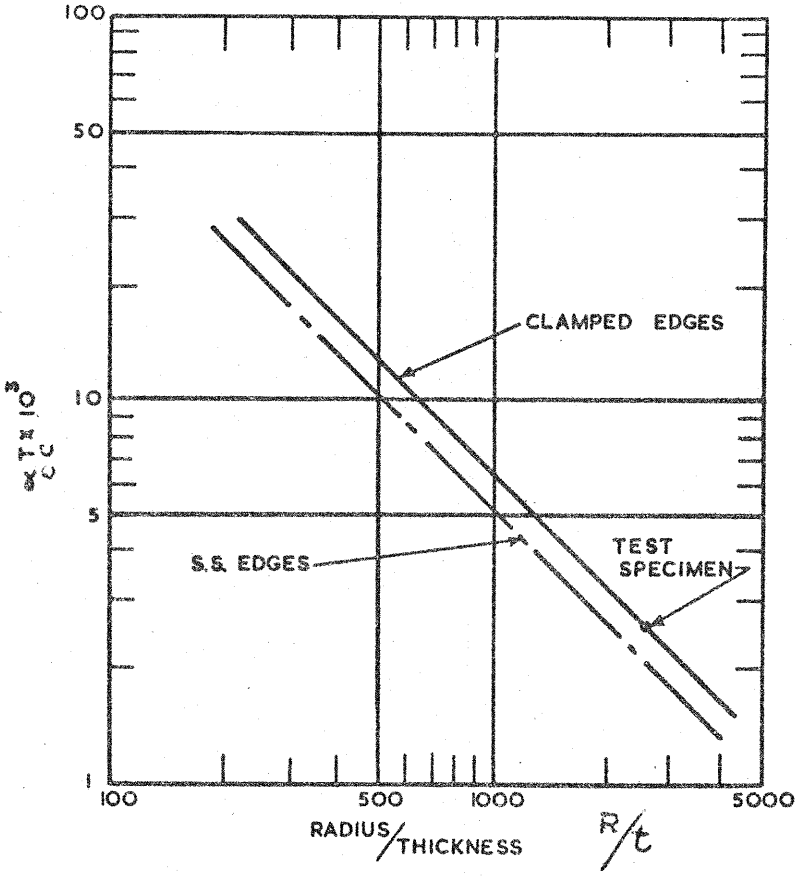

FIG. 19. BUCKLING OF CIRCULAR CYLINDERS DUE TO UNIFORM SHELL TEMPERATURE RISE

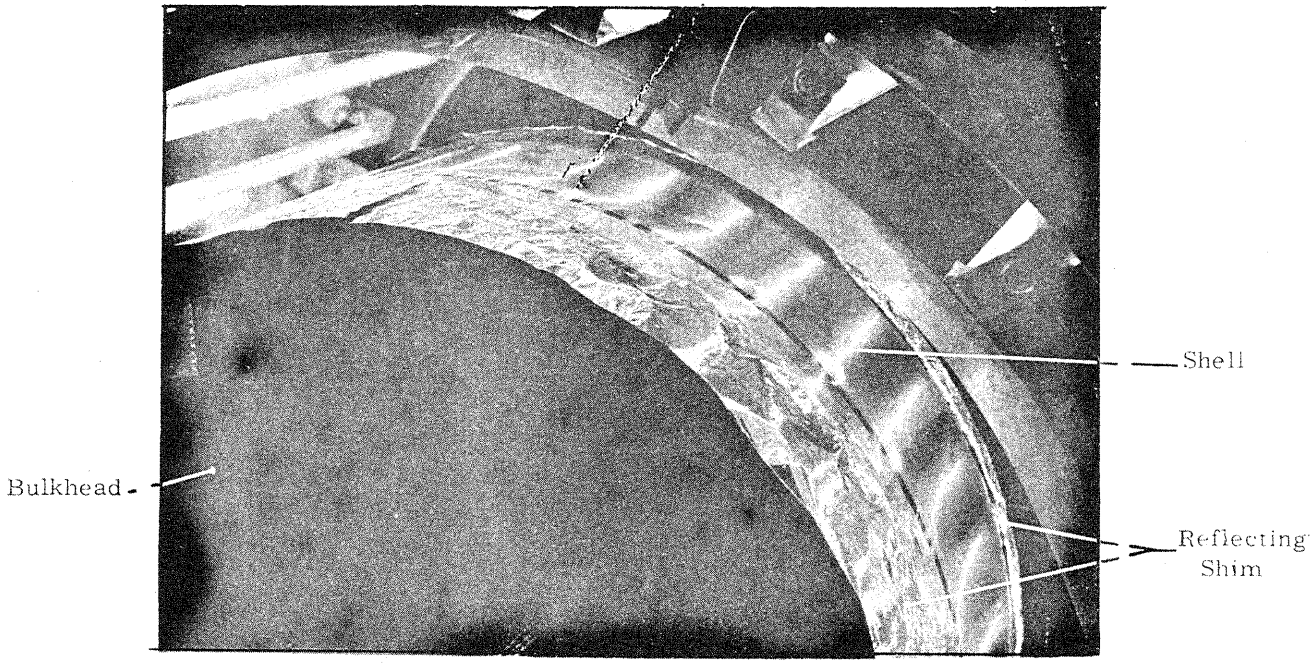

FIG. 20. THERMAL BUCKLES DUE TO DISCONTINUITY STRESSES IN A THIN CYLINDRICAL SHELL

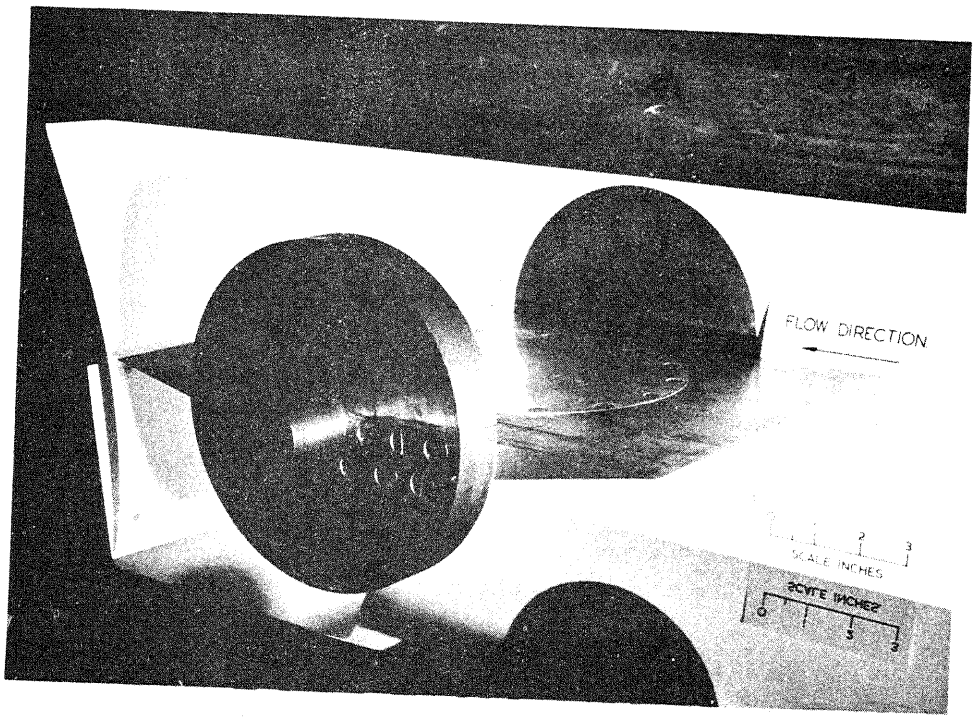

FIG. 21. FLUTTER MODEL MOUNTED IN TUNNEL
(ONE WALL REMOVED)

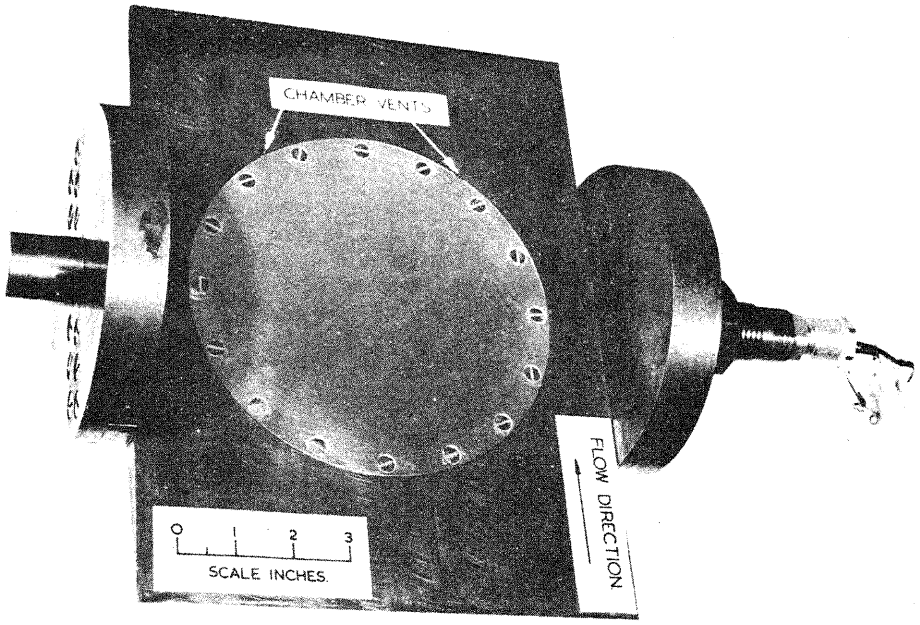

FIG. 22. VIEW ON UPPER SURFACE OF FLUTTER
MODEL WEDGE

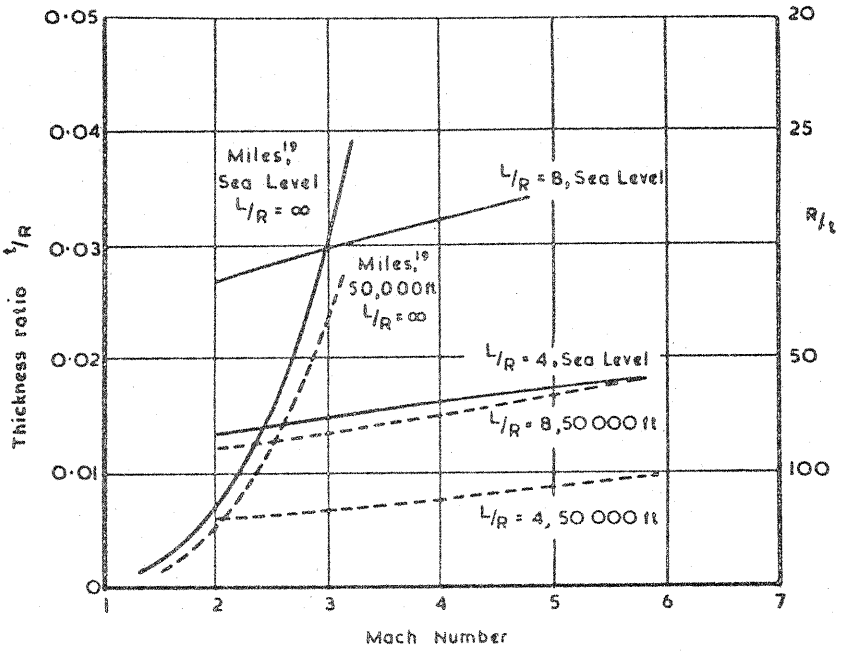

FIG. 23. THICKNESS REQUIRED TO PREVENT FLUTTER FOR AN EMPTY STEEL CYLINDER AT SEA LEVEL IN THE CASE n = 0. FRONT EDGE CLAMPED, REAR EDGE SIMPLY SUPPORTED. n = NUMBER OF CIRCUMFERENTIAL WAVES

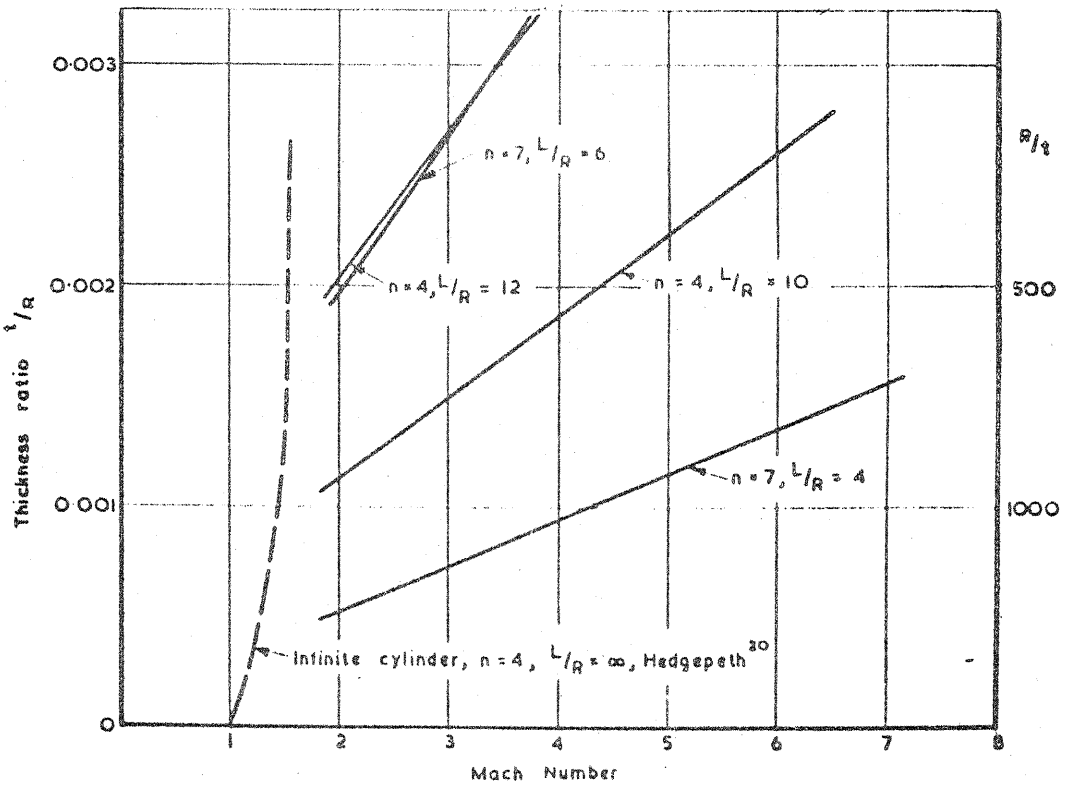

FIG. 24. THICKNESS REQUIREMENT TO PREVENT FLUTTER FOR AN EMPTY STEEL CYLINDER AT SEA LEVEL IN THE CASE $n \neq 0$. FRONT EDGE CLAMPED, REAR EDGE SIMPLY SUPPORTED, n = NUMBER OF CIRCUMFERENTIAL WAVES

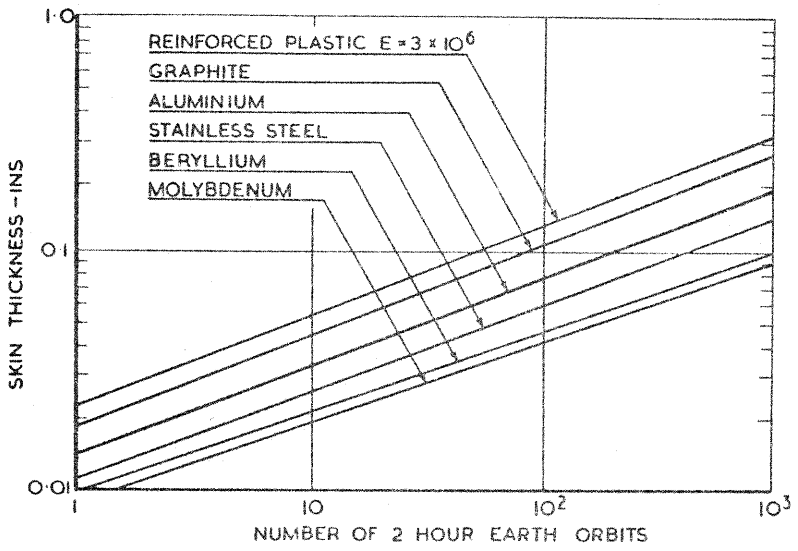

FIG. 25. REQUIRED WALL THICKNESS FOR METEOROID PROTECTION

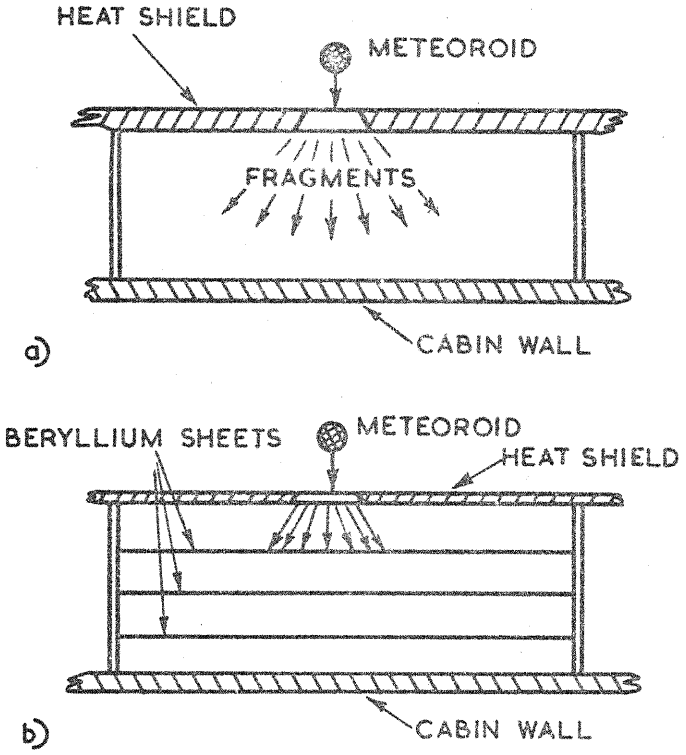

FIG. 26. METEOROID BUMPERS

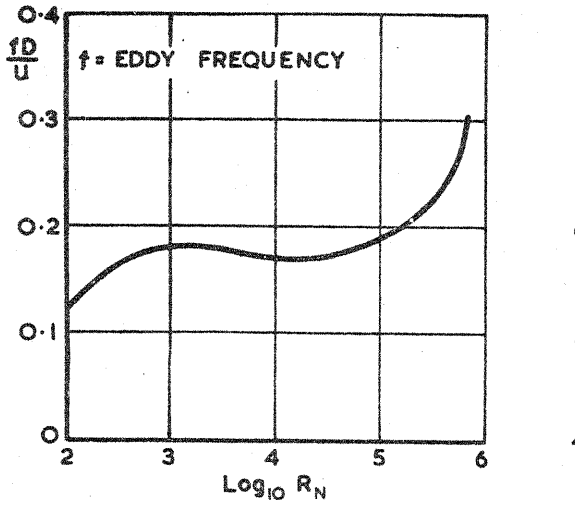

FIG. 27(a). DEPENDENCE OF STROUHAL NO. ON REYNOLDS NO. FOR A CIRCULAR CYLINDER

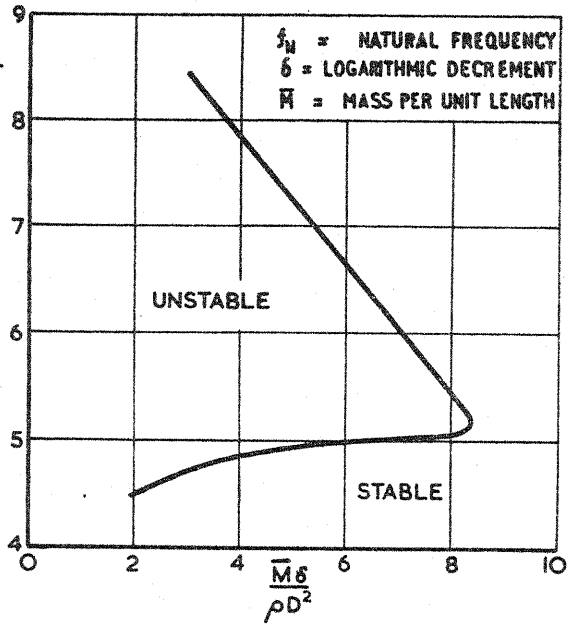

FIG. 27(b). AERODYNAMIC STABILITY DIAGRAM FOR CIRCULAR CYLINDRICAL CANTILEVERED ROD

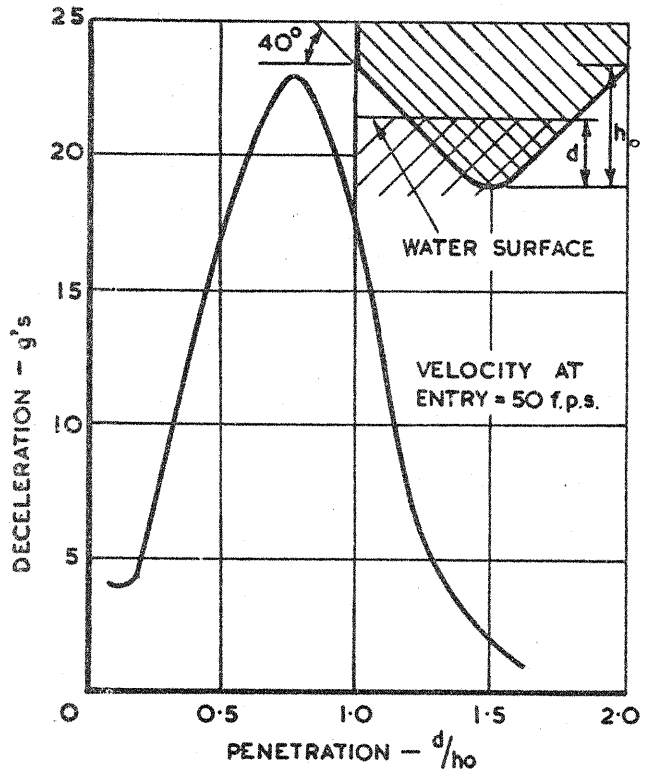

FIG. 28. RIGID BODY IMPACT LOADS DURING WATER ENTRY

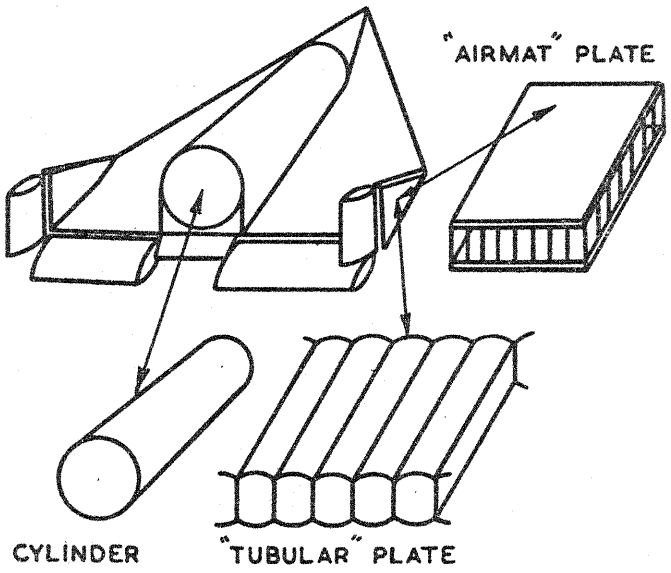

FIG. 29. TYPICAL INFLATABLE CONFIGURATION

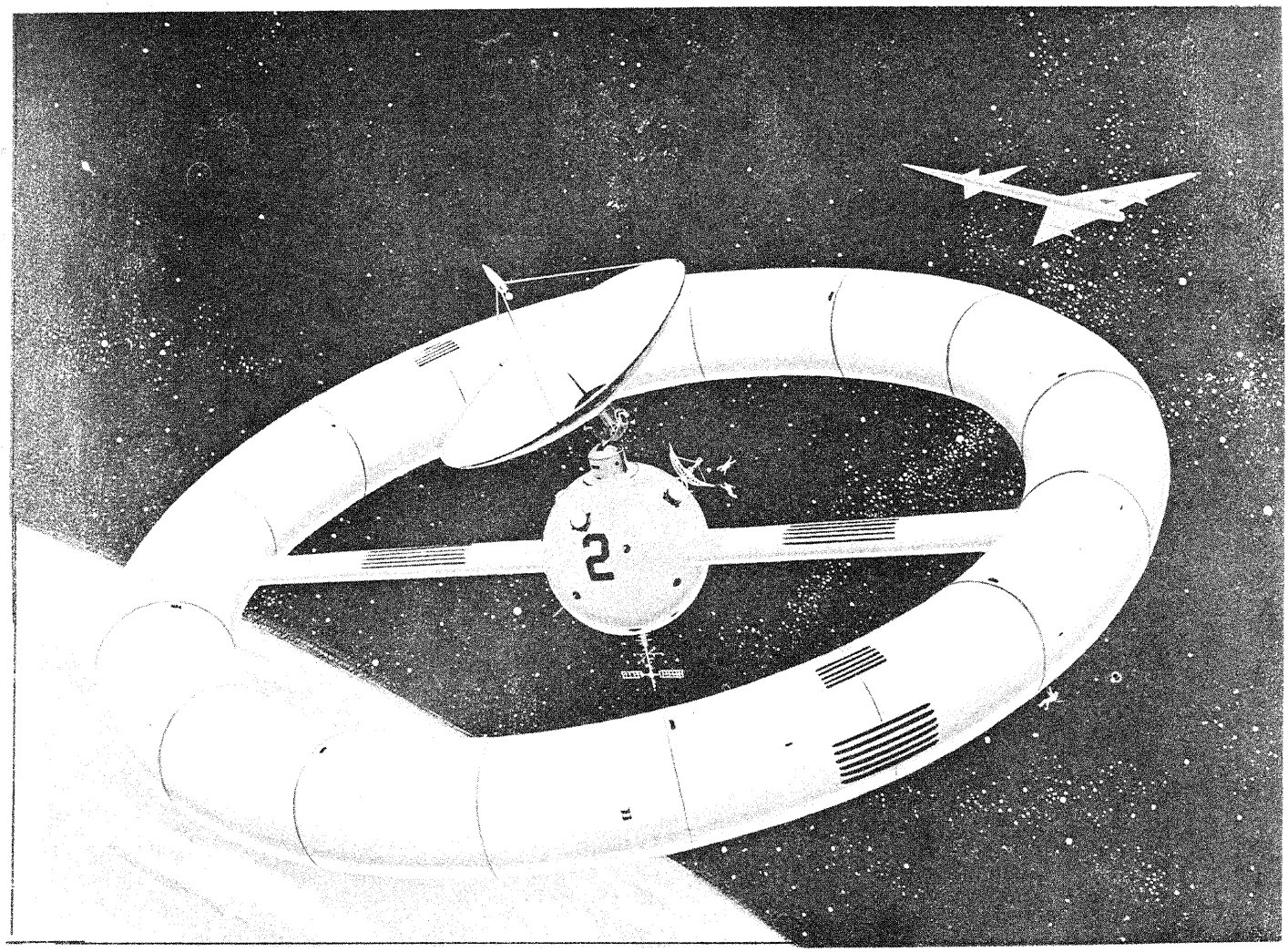

FIG. 30. A GOODYEAR DESIGNED INFLATED SPACE STRUCTURE

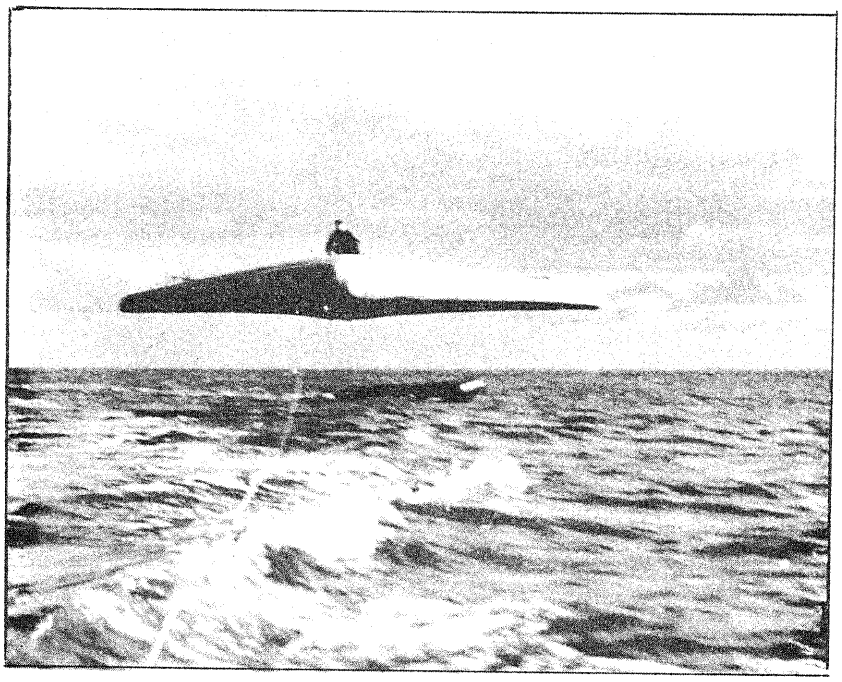

FIG. 31. AN INFLATED GLIDER

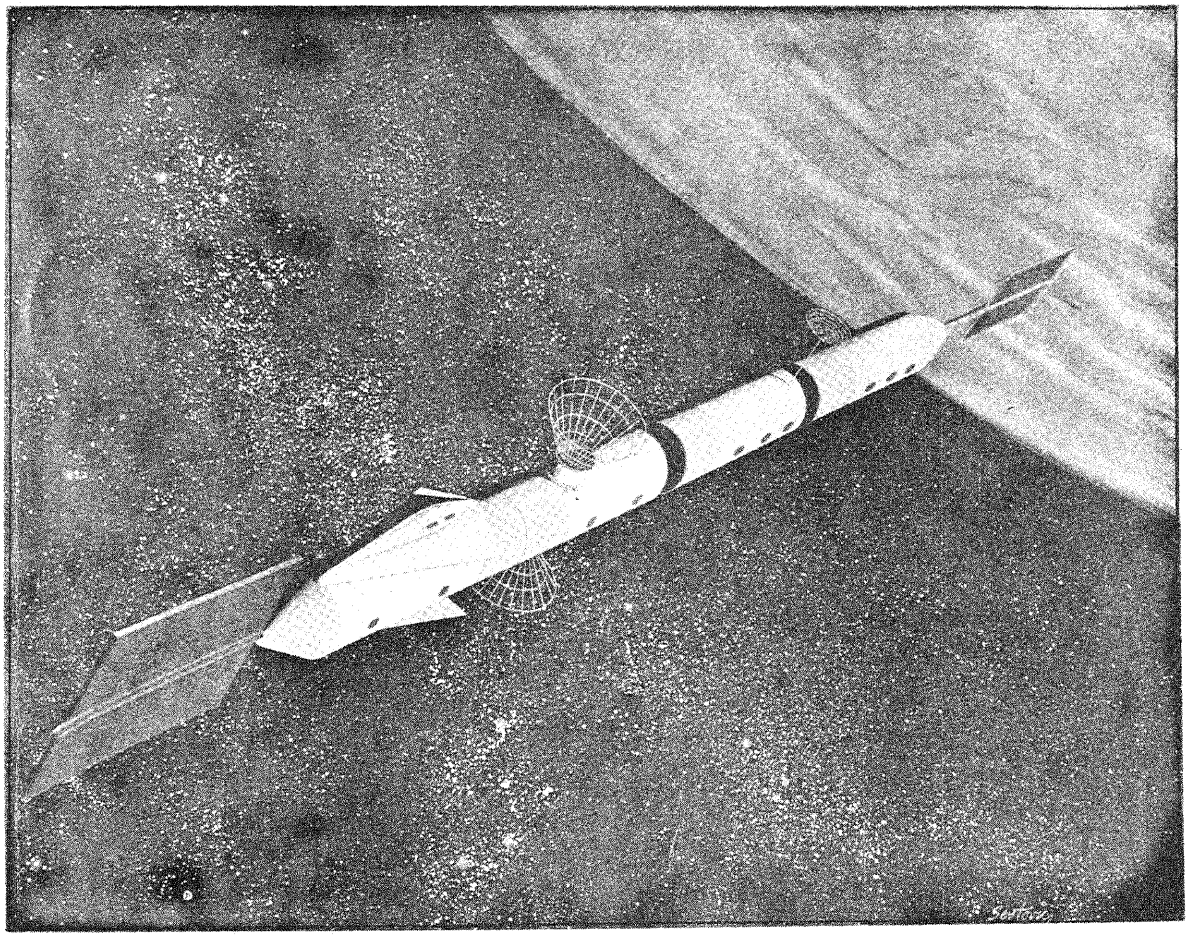

FIG. 32. A MANNED SPACE STATION DESIGN UTILISING PROPELLANT TANKAGE (CONVAIR ASTRONAUTICS)

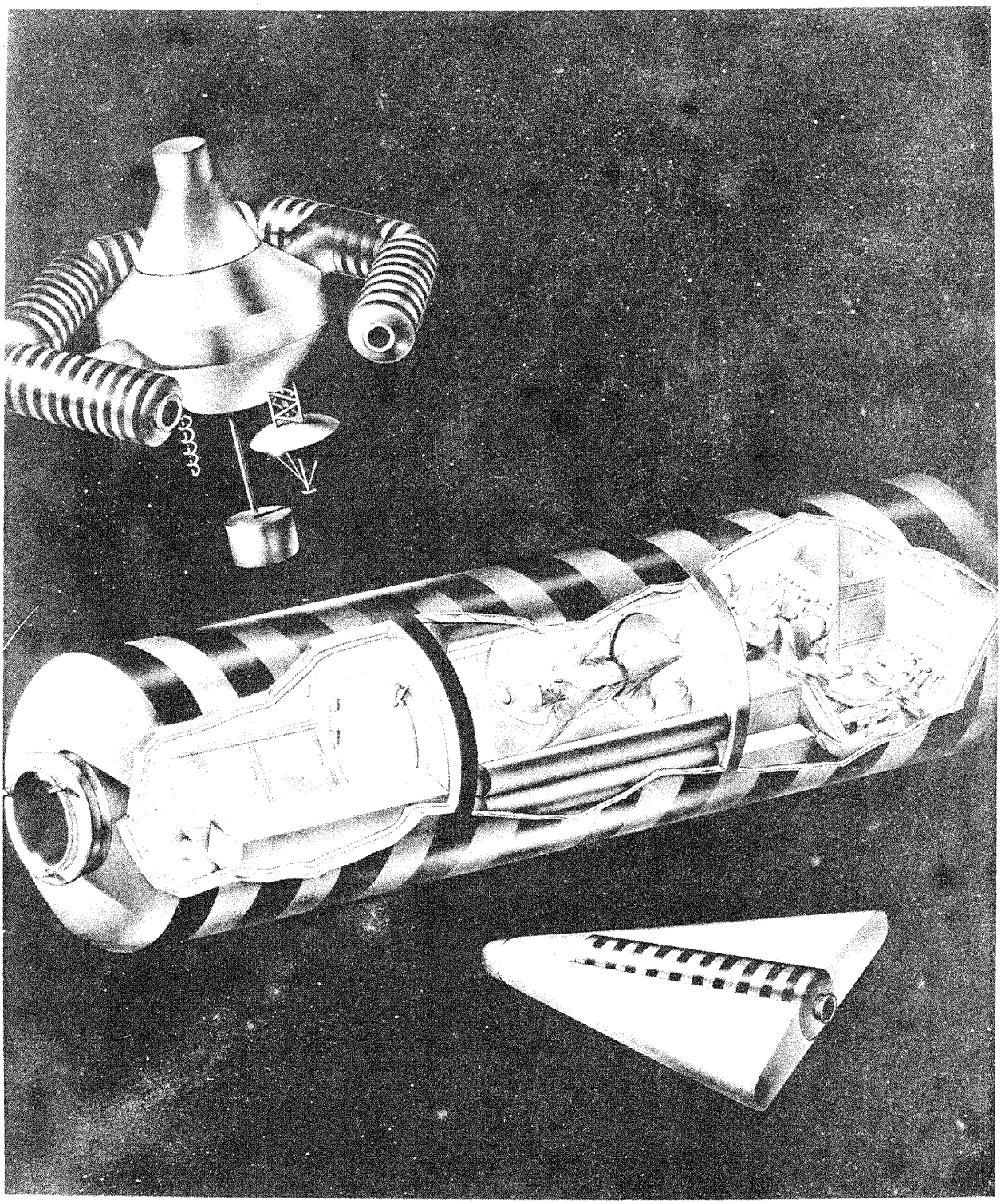

FIG. 33. APPLICATIONS OF DOUBLE WALL SPACE STRUCTURE (FORD AERONUTRONIC)

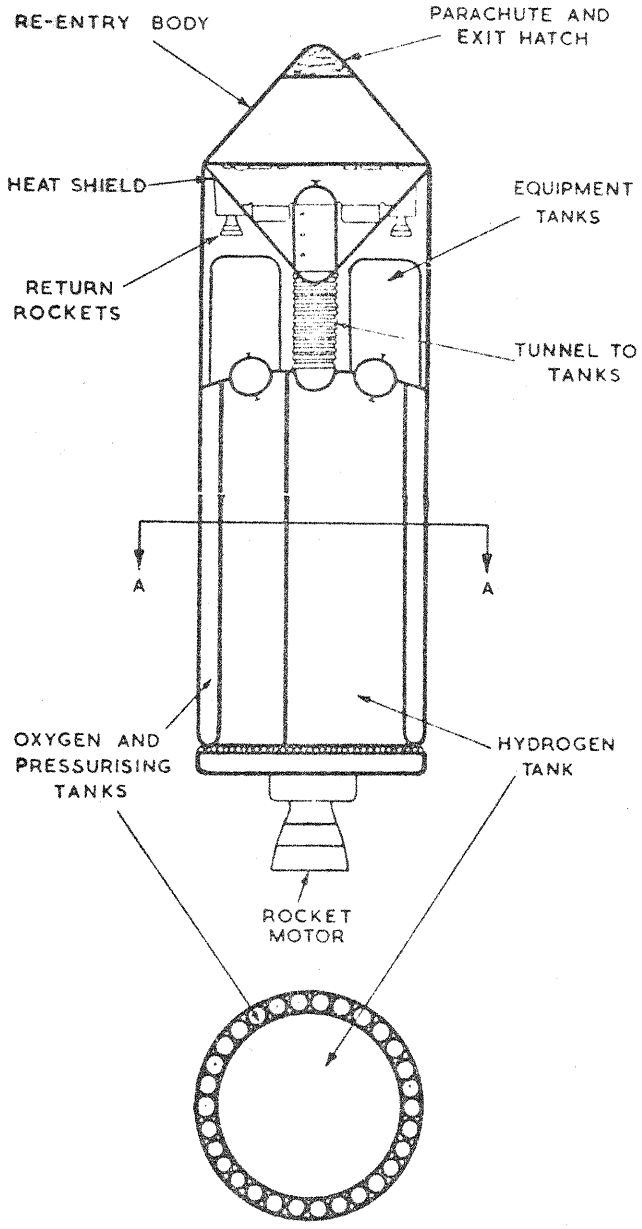

FIG. 34. SPACE VEHICLE. PRINCIPAL FEATURES